To the Graduate Council:

I am submitting herewith a thesis written by Shen Zhu entitled "**Excited-State Properties of DNA**". I have examined the final copy of this thesis for form and content and recommend that it be accepted in partial fulfillment of the requirements for the degree of Master of Science, with a major in Physics.

Solon Georghiou, Major Professor

We have read this thesis
and recommend its acceptance:

Accepted for the Council:

Vice-Chancellor
and Dean of the Graduate School

EXCITED-STATE PROPERTIES OF DNA

A

Thesis

Presented for the

Master of Science Degree

The University of Tennessee, Knoxville

Shen Zhu

December 1990

ACKNOWLEDGEMENTS

I would like to thank Dr. S. Georghiou for his patient guidance during this study and Dr. R. Weidner for introducing me to the stochastic theory. I am grateful to Dr. Chao-Ran Huang for carrying out the methylation of DNA and to Mr. Guangyuan Ge for the measurements on 7-methyl GMP and methylated DNA; I originally carried out measurments on 7-methyl GMP in glycerol, but, as I explained in Chapter 2, we found it more appropriate to use aqueous solutions instead. I would also like to thank Mr. T. Bradrick for very helpful discussions on the excited-state properties of 7-methyl GMP and for technical assistance.

I would also like to thank the Department of Physics of the University of Tennessee for a teaching assistantship during the course of these studies.

This research was supported by Research Grant GM38236 from the National Institutes of Health.

ABSTRACT

In this thesis I discuss the properties of the excited electronic states in mehtylated DNA and its bases.

In the first part I describe steady-state measurements of fluorescence anisotropy in order to resolve the long-wavelength absoption spectrum of 7-methyl GMP in pH 5 buffer at room temperature into component spectra that correspond to the electronic transitions I and II present in that spectral region. We have chosen this derivative of guanine because its fluorescence quantum yield is much greater than that of GMP. It is found that the data are adequately described by a model that involves emission exclusively from state I, with state II converting to it with 100% efficiency. The shape of the absorption spectrum of state II is virtually independent of the angle θ between the absorption transition dipole moments of states I and II, whereas that of state I is dependent on θ. We analyze the data on the basis of the premise that in the short-wavelength region state II is the predominantly absorbing state. This premise is based on studies of single-crystal polarized reflection and linear dichroism from stretched films. The spectral maxima for the two states are found to be at about 290 nm and 260 nm, respectively. There is also a weak band which is centered at about 245 nm. The oscillator strengths are found to be 0.07, 0.21 and ≈ 0.04, for states I, II and that associated with the weak band, respectively. The importance of these findings with regard to the photophysical properties of nucleic acids and calculations of their CD spectra is discussed.

In the second part, I report the results of a study in which an irreversible electronic energy trap has been formed in calf thymus DNA by methylating about 75% of its G bases at position N-7. This has allowed us to measure for the first time the efficiency of transfer of energy along the helix of a double-stranded nucleic acid at room temperature. It is found that about one out of every three photons absorbed by the other bases is trapped. We have also simulated the data with a stochastic model that uses the dipole-dipole interaction to calculate the efficiency of transfer. In order to approximate the experimental results, the model requires that: (i) the fluorescence quantum yield of T, C, and G in

DNA be about 2×10^{-3}, which is about two orders of magnitude larger that the value of the fluorescence quantum yield reported for DNA; and (ii) the fluorescence quantum yield of A in DNA be negligibly small. Requirement (i) is consistent with energy transfer taking place before a very efficient fluorescence quenching process sets in, which could be formation of excited-state complexes (excimers) that do not fluoresce appreciably. Requirement (ii) implies a very short fluorescence lifetime for A, which is consistent with the reported absence of a significant number of photoproducts formed by A in DNA. The simulations find that, on the average, the excitation energy takes about 1.2 steps to reach the trap; that is to say, bases that are nearest and next nearest neighbors of the trap are, in effect, the only energy donors. Both intra- as well as interstrand energy transfer (the latter only for the C-trap base pair) make significant contributions. The values of the efficiency for pairwise base-base intrastrand transfer are 90% and 80%, respectively. The corresponding values for the rate constant of transfer are 2×10^{11}, 1×10^{12}, and $4 \times 10^{11}\ s^{-1}$. Transfer is inefficient when A is the donor or the acceptor. In addition to the dipole-dipole term, the only other significant term in the expansion of the interaction potential is the dipole-quadrupole term which, however, makes only a small contribution to the overall transfer efficiency. The electron exchange interaction appears to be much less efficient than the coulombic interaction.

TABLE OF CONTENTS

LIST OF FIGURES

FIGURE **PAGE**

Chapter 1

INTRODUCTION

Since Watson and Crick[1] reported the remarkable double helix model of DNA, much work has been done to try to gain more understanding of the structure and properties of DNA. Until now, understanding the properties of the electronic states still is a goal for further research. Although a number of experiments has been done in low temperatures, knowledge about the structure and dynamics of excited states of DNA is fragmented and incomplete [2]. In recent years, DNA has been studied more and more at room temperature because of the availability of inexpensive and high purity samples. [3–5]

Luminescence spectroscopy of nucleic acids is a very useful technique that yields information regarding the mechanisms of the effects of UV radiation on cells. Also, information on the direction of the transition dipole moments of their electronic states contributes toward more realistic calculations of CD spectra; the latter are very sensitive indicators of nucleic acid conformation. Moreover, time-resolved polarized emission studies have the potential for elucidating the conformational flexibility of nucleic acids, a property that plays an important role in their function.

Nucleic acids at room temperature under physiological conditions fluoresce very weakly, however, and this makes such measurements very difficult to carry out. Nevertheless, considerable progress has been made, reviewed by Callis[2]. Early work at low temperature was reviewed by Gueron et al[6].

Here, I discuss some properties of nucleic acids in their excited states. We methylated guanine at position N-7 in order to increase its fluores-

cence quantum yield. We have chosen this derivative of guanine because its fluorescence quantum yield is much greater than that of GMP. It is found that the data are adequately described by a model that involves emission exclusively from state I, with state II converting to it with 100% efficiency. We also methylated the guanine bases in DNA. This has allowed us to measure for the first time the efficiency of transfer of energy along the helix of a double-stranded nucleic acid at room temperature. It is found that about one out of every three photons absorbed by the other bases is trapped by the methylated bases. We have also simulated the data with a stochastic model that uses the dipole-dipole interaction to calculate the efficiency of transfer.

1.1 Transition Dipole Moments

DNA has a double helical structure which is very stable. There are three kinds of forces that stabilize the DNA double helix. One is the hydrogen bond between the base pairs; A-T and C-G form the two types of base pairs in DNA. There are three hydrogen bonds in a C-G base-pair and two hydrogen bones in a T-A base-pair. The second force is interaction between the phosphate groups which have a negative charge and positive ions in solution. The strongest force that maintains the stability of DNA stems from stacking interactions between the π electrons of the bases. The calculation for the $\pi\pi^{\star}$ interaction is very complicated. Some good calculations[7–11] were done only for pyrimidine DNA bases, thymine (uracil) and cytosine. For purine DNA bases still there are no satisfactory results.

From early CD studies done by Sprecher and Johnson[12] and later UV experiments[13], some evidence shows the strong transition moments lying in the plane of the bases. The out-of-plane transition moments are weaker than those in the plane[2]. In the long-wavelength band Stewart and co-workers[14] using a 9-methyadenine single crystal found the transition moments for band I and band II to be -3^o and 45^o, respectively. The very different value of 89^o for band I has been recently reported by Clark[15]. This is the value I used in my calculations with the stochastic

model. Most experiments have indicated that the thymine base has only one transition moment at 260 nm band, and the transition moment is found to be at -19° [16,17]. Information regarding the transition moments of cytosine base came from the experiments done by Callis and Simpson[18] on polarized reflection, and those of Lewis and Eaton[19] on absorption for single crystals. They found that there are two directions of the transition moments; for band I (270 nm) it is 14° and for band II (235 nm) it is 25°. The direction of 14° will be used in my calculations for the DNA stochastic model, because the excited state of band I is lower than that of band II. Guanine also has two electronic excited states. We found two electronic excited states in 7-methyl GMP, but only band I emits and band II converts 100% to band I. The orientation of the two bands at long wavelengths has an angle of about 45° which is different from the angle between the transition moments of the two bands which was reported to be between 70° and 90° for guanine and some of its derivatives[2]. I will give possible reasons for this disagreement in Chapter 2. The results for guanine hydrochloride favor the $-4°$ value[20] for band I, and the long-axis assignment for II is confirmed[13].

1.2 Recent Studies at Room Temperature

Scientists have been working on monomers, dinucleosides and polynucleosides for several decades at low temperature conditions. Naturally, researchers are more interested in doing experiments at room temperature, which is closer to the physiological temperature. About twenty years after Watson and Crick proposed their model on the DNA structure, Daniels and Hauswirth[4,5] did the first room temperature experiment in 1971. They reported the fluorecence spectra, excitation spectra, and the fluorescence polarization for monomers. They found that the fluorescence quantum yield of a common base is of the order of 10^{-4}. Soon after that, Vigny and co-workers[3,21–23] published several papers in which they discussed the properties of dinucleosides and polynucleosides at room temperature. They found that the fluorescence quantum yields of dinucleosides and polynucleosides are also of the order of 10^{-4}. They

also reported that there are both monomeric and excimeric contributions in the fluorescence spectra of some dinucleotides as well as single- and double-stranded polynucleotides. Of special interest are the results for the alternating polynucleotide poly(dA-dT)·poly(dA-dT). By varying the temperature, these authors obtained strong evidence for excimeric emission, for which the band has a maximum at about 410 nm[21]. Many properties of the electronic states, however, for common bases and DNA are still not well understood.

1.3 The Present Study

In order to understand the excited-state properties of DNA, it is important that the excited-state properties of the individual nucleotides are first understood. Guanine is a particularly complicated case, since in its long-wavelength absorption spectrum there are two electronic states. Clark[20] analyzed graphically the absorption spectrum by using gaussians. We attempted to resolve the absorption spectrum in a unique way by measuring the emission anisotropy of 7-methyl GMP as a function of excitation wavelength. This study allowed us to show that the upper electronic state converts to the lower state with 100% efficiency. The lower state is the only one that emits. Interestingly, we found that the individual absorption spectra overlap considerably each other and have vibronic structure. We discuss the lattter property with regard to energy transfer between vibronic levels.

Virtually nothing is known about singlet-singlet energy transfer in DNA. Ballini and co-workers discussed energy transfer in tRNA[24]. They used the spectroscopic properties of the odd nucleoside 4-thiouridine, which is present in position 8 of 70% of E. coli tRNAs, to study intermolecular energy transfer. The measurements of the luminescence excitation spectrum and action spectrum were done at room temperature in native E. coli tRNA. They found that energy transfer does occur from the common nucleotides to the 4-thiouridine residue, and reported that 80% of energy transfer comes from the guanosine and cytidine residues. We are concerned with energy transfer in DNA. Due to thermal fluctuations,

the hydrogen bond may be broken. An excited base whose hydrogen bond is broken could form a photoproduct with an adjacent base. The probability of forming a photoproduct will increase when energy transfer in DNA occurs before hydrogen bonds are reformed. Since the fluorescence of DNA is so weak, we chose the methylated DNA which is much more fluorescent than DNA, and which still has a B comformation. The methylated guanines play the role of an irreversible energy trap. This process was not observed before, and so there is no model available. We set up a stochastic model to simulate energy transfer in the DNA double helix. In this model, the rates of energy transfer were calculated from the dipole-dipole interaction. We foud that energy transfer takes place before excimers are formed. The most important contribution of energy transfer comes from thymine and cytosine. Only few photons are transferred from adenine and guanine which is only 5% of the DNA bases. From this model, we also found that energy transfer almost takes place exclusively between nearest bases: the number of steps needed for the energy to reach the trap is about 1.2. We also learned from this study that energy transfer takes place before a very efficient radiationless process takes place in the bases, which results in a very large reduction in their fluorescence.

Chapter 2

TWO ELECTRONIC STATES IN 7-METHYL GMP

In the long-wavelength absorption band (wavelengths longer than about 240 nm) there is only one transition for thymine and cytosine and two nearly degenerate transitions for adenine. As for guanine and its derivatives, studies of polarized reflection from single crystals[20,25] and linear dichroism from stretched films[26] showed that there are two transitions I and II that are approximately perpendicular to each other. Thus, in order to delineate the photophysical and photochemical properties of guanine, it is necessary that its absorption spectrum be resolved into its two component spectra. Such information is also necessary for calculating the CD spectra of nucleic acids.

Here, I report the results of a study that accomplished these objectives by employing steady-state fluorescence anisotropy and quantum yield measurements for 7-methyl GMP in a pH 5 buffer. We have chosen this derivative of guanine because it has a fluorescence quantum yield about 150 times greater than that of GMP[21,27,28]. The data are found to be adequately described by a model which involves conversion of state II to state I with 100% efficiency and emission exclusively from state I. States I and II are found to have spectral maxima at about 290 nm and 260 nm, respectively.

2.1 Materials and Methods

7-methyl GMP, chromatographically pure, was obtained from Sigma (st. Louis, MO). Sodium chloride and sodium cacodylate were obtained from Fisher Scientifc (Springfie;d, NJ) and BDH (Dorset, England), respectively. Cyclohesane was a product of Mallinckrodt (supplied by Scientific products, Mcgraw Park, IL), whereas p-terphenyl was a scintillation-grade product of K&K Laboratories (Plainview, NY).

Absorption measurements were made on a Shimadzu UV-265 spectrophotometer (Columbia, MD). Fluorescence anisotropy measurements were taken with a spectrofluorometer that employs a 1 kW Xe-Hg light source (Spectral Energy Corp., Hillsdale, NJ), two 0.5 m focal length Barsch and Lomb monochromators (Rochester, NJ), a thermoelectrically cooled 9558 QB EMI photomultiplier (Fairfield, NJ) and a Stanford Research Systems SR440 preamplifier and SR400 photon counter (Sunnyvale, CA). A 3M 105-UV-WRMR polarizer (ST. Paul, MN) was placed in the excitation light path and an HNP'B polarizer (Cambridge, MA) in the emission path. The fluorescence anisotropy, r, was calculated from

$$r = \frac{I_{VV} - I_{VH}(I_{HV}/I_{HH})}{I_{VV} + 2I_{VH}(I_{HV}/I_{HH})} \tag{2.1}$$

where I is the fluorescence intensity, V and H stand for vertical and horizontal orientation, respectively, and the first subscript refers to the excitation polarizer while the second refers to the emission polarizer. For the plot of the anisotropy as a function of excitation wavelength, the bandwidths for excitation and emission were 1.7 and 5 nm, respectively. These as well as all the other fluorescence measurements in this study were made at room temperature with samples that had a maximum absorbance of 0.05 at 258 nm.

The values of the relative fluorescence quantum yield for 7-methyl GMP were corrected for the variation of the exciting light intensity with excitation wavelengh. Correction factors were determined from a measurement of the excitation spectrum of p-terphenyl in cyclohexane. The excitation and emission bandwiths were 1 nm and 3.3 nm, respectively.

Fluorescence spectra were measured with excitation and emission bandwidths of 5 nm and 0.5 nm, respectively; they were corrected for the variation of the sensitivity of the photomultiplier-monochromator combination with emission wavelength employing a standard lamp[29].

The buffer consisted of 0.05 M sodium cacodylate, 0.1 M NaCl, pH5 (in triply distilled water). This pH was used to ensure that the proton at N_1 of 7-methyl GMP is not dissociated ($pk_a = 7.1$[30],) and, therefore, there is no contribution to emission from an ionized species. A correction was made for buffer contribution to emission.

2.2 Results and Discussion

As part of our study of the excited-state properties of 7-methyl GMP at room temperature, we previously reported that its degree of fluorescence polarization is much lower when exciting at 265 nm than when exciting at longer wavelengths[28]. An earlier study[31] reported a similar behavior for guanine. These findings and the reported presence of two electronic transitions in its long-wavelength absoption band[20,25,26] prompted us to undertake a more detailed study across the absorption band. Figure 1 (all of Figures in Appendix VI) shows a plot of the fluorescence anisotropy r of 7-methyl GMP as a function of the excitation wavelength. It is seen that r is high at long wavelengths, decreases steadily at shorter wavelengths, and increases slightly below 260 nm.

In order to analyze these data, the dependence of the fluorescence quantum yield on the excitation wavelength must be known. In the present study we found that the quantum yield exhibits no such dependence (Fig. 2). In our group initial study[28] we found the fluorescence quantum yield of 7-methyl GMP at pH 5 to vary somewhat in the spectral region of 280 to 305 nm. Improvements in the sensitivity of our spectrofluorometer have now resulted in a much more accurate determination of the fluorescence quantum yield as a function of excitation wavelength. Also, we found that the fluorescence spectrum (Fig. 3) does not depend on the excitation wavelength when exciting in the 240 nm to 310 nm spectral range. Moreover, we found the fluorescence anisotropy

to be independent of the emission wavelength (data not show).

These findings are consistent with emission from only one of the two states. Below we test such a model as to how well it describes the fluorescence anisotropy data. The subscripts a and b will refer to the electronic states I and II, respectively.

The model considers emission to originate exclusively from state I, with state II converting to I with an efficiency of 100%. (This requirement is dictated by our finding that the fluorescence quantum yield is independent of the excitation wavelength, Fig. 2). We shall assume that excitation at 310 nm exclusively populates state I that has emission anisotropy r_a. That the anisotropy is seen from Fig. 1 to reach a maximum and approximately constant value in the 306 nm to 314 nm spectral range provides support for this assignment. From Fig. 1, $r_a \approx 0.080$.

The apparent anisotropy r at any excitation wavelength is

$$r = f_a r_a + f_b r_b \tag{2.2}$$

where f_a and f_b are the fractions of light absorbed by states I and II, respectively, and r_b is the anisotropy when exciting state II. Noting that

$$f_b = 1 - f_a \tag{2.3}$$

we obtain from (2.2)

$$f_a = (r - r_b)/(r_a - r_b) \tag{2.4}$$

For every excitation wavelength the fraction of light f_a absorbed by state I is obtained from Eq. (2.4). (See Eq. (2.8) below as to how r_b is determined.) The fraction of light f_b absorbed by state II is subsequently obtained from Eq. (2.3). The absorbances A_a and A_b for states I and II, respectively, are then obtained from

$$A_a = f_a A, A_b = f_b A \tag{2.5}$$

where A is the total absorbance at that wavelength. Below, we find that this model describes the data adequately.

As we stated above, we assume that absorption at long wavelengths excites state I exclusively. The emission anisotropy r_a of that state is

approximately equal to 0.08. If the fluorescence depolarization is due to rotational diffusion during the lifetime of the excited state, then the Perrin equation[32,33] yields

$$r_a/r_{max} = \frac{\phi}{\phi + \tau} = P_2(< cos\alpha >). \tag{2.6}$$

Here $< cos\alpha >$ is the average value of the cosine of the angle between the absorption and emission transition dipole moments of state I, P_2 is the Legendre polynomial of order two, τ is the fluorescence decay time, ϕ is the rotational correlation time and $r_{max} = 0.4$ is the maximum anisotropy. This equation yields $P_2(< cos\alpha >) = 0.2$ or $\tau/\phi = 4$, which for $\tau = 180$ ps[34] gives a value for ϕ of 45 ps. Thus, extensive rotational diffusion takes place during the lifetime of the excited state. We note in this regard that we chose to use aqueous buffer rather than glycerol as the solvent despite the fact that the values of r can be more accurately measured in the latter than in the former. We did this in order to avoid complications that arise when exciting at long wavelengths. Indeed, we found the fluorescence spectrum and fluorescence quantum yield to vary with the exciting wavelength in that spectral range in glycerol in which we had 0.2 M HCI so that 7-methyl GMP is protonated. These complications stem from the presence of heterogeneity in the microenvironment of the emitting molecules in this highly viscous solvent. (This is the so-called red-edge effect, see Demchenko and Ladokhin[35] for a recent account.) For this same reason we did not carry out the measurements at low temperature either.

In the case of excitation of state II , absorption is followed by a rapid relaxation to state I, which then undergoes rotational diffusion while it fluoresces. By taking the steady-state average of the time-dependent anisotropy derived by Tao[36] for this case, we obtain the following expression for the anisotropy r_b of state II

$$r_b = 0.4P_2(< cos\alpha >) \times P_2(cos\theta). \tag{2.7}$$

Here, θ is the angle subtended by the absorption transition dipole mo-

ments of states I and II. By combining Eqs. (2.6) and (2.7), we obtain

$$r_b = 0.08P_2(cos\theta) = 0.08(\frac{3cos^2\theta - 1}{2}). \qquad (2.8)$$

(We note that Eq. (2.6) is still valid if the depolarization of the fluorescence of state I is caused not only by rotational diffusion but by some fast reorientation process as well.)

No values for the angle θ between the transition dipole moments of states I and II have been reported for 7-methyl GMP or, for that matter, for GMP or guanosine. The only values reported are for guanine hydrochloride, 9-ethyl guanine and guanine, and these come from studies of polarized reflection from single crystals[20,25] and linear dichroism from stretched poly(vinyl alcohol) films[26]. For guanine and for guanine hydrochloride[20] θ was found to be close to 90^o. However, ethyl substitution at position 9 of guanine was found to reduce θ to about 60^o [25], while another study yielded about 70^o [20]. Sugar substitution at position 9 also appears to reduce θ as judged from the observation that guanosine exhibits a very different reduced dichroism profile from that exhibited by guanine[26]. (As the authors point out, a more complex orientation distribution brought about by the introduction of the ribose group may also contribute to the change in the profile.) The question, of course, arises as to whether methylation at position 7 causes a large change in θ. The aforementioned observation that for guanine hydrochloride which is protonated at position 7 the value of θ is very similar to that for guanine implies that the introduction of a positive charge does not have a significant effect on the directions of the absorption transition dipole moments of states I and II. It would, therefore, appear that the positive charge introduced by methylation does not greatly affect θ. The possibility that the presence of the methyl group itself alters θ cannot, of course, be excluded. Despite this uncertainty, we chose 7-methyl GMP because its fluorescence quantum yield is about 150 times greater than that of GMP[21,27,28]. Indeed, as a result of the very low room-temperature fluorescence quantum yield of guanine, its fluorescence anisotropy could not be accurately determined below 260 nm[31], where the exciting light intensity is quite low. In addition, as we mentioned above, there is no

information regarding θ for GMP or guanosine, which would have been the most appropriate choice for study in the present work. Guanine, for which θ was found to be about 90^o [26], is not a good choice either because of the occurrence of $7 \longleftrightarrow 9$ tautomerism that renders the state of its ionization uncertain.

The limitations of the methods used to determine θ also need to be considered in this discussion. The analysis of polarized single-crystal reflection data is in general somewhat ambiguous because of its neglect of intermolecular interactions[37–39]. For linear dichroism studies of small, nonsymmetrical molecules there are uncertainties associated with determining the order parameters. Thus, the values for θ determined by both methods should be considered to be approximate. Calculations[40–42] of the directions of the transition dipole moments of states I and II unfortunately are not very helpful in this regard, for their agreement with experiments is poor.

In view of these considerations, we examine below the sensitivity of the analysis of the fluorescence anisotropy data (Fig. 1) to the value of θ. Appendix 1 shows the values of the fraction of light f_a absorbed by state I at 290, 260 and 244 nm as a function of θ. It is seen that at 290 nm absorption by state I predominates for all values of θ. On the other hand, at 260 nm absorption by state II predominates for $\theta < 50^o$. Upon going from 50^o to 40^o, f_a decreases sharply, by about 500%. For $\theta \leq 40^o$, f_a actually attains negative values, which implies that such θ values are not physically meaningful. The increase of the anisotropy below 260 nm (Fig. 1) demands that state I (or some other state whose polarization is similar to that of state I) make a significant contribution in that spectral range. This is borne out by the values of f_a at 244 nm (Appendix 1). In summary, although at long wavelengths state I predominates regardless of the value of θ, for state II to predominte at short wavelengths, θ must be less than 50^o. Values of θ less than about 40^o are not feasible.

Figures 4 and 5 show the total absorption spectrum and the constituent absorption spectra for states I and II obtained by the analysis described above for $\theta = 70^o$ and $\theta = 43^o$, respectively. We chose these two angles in order to illustrate how the spectra look (i) when absorption

by state I predominates across the total wavelength range (Fig. 4) and (ii) in the other case, when absorption by state II predominates at short wavelengths, and absorption by state I predominates at long wavelengths (Fig. 5). We note that with regard to Fig. 4, we found f_a to be quite insensitive to the value of θ in the range of 70^o to 90^o (figures not shown): e.g., for the three wavelengths shown in Appendix 1, f_a increases by less than 10% in this range of value for θ. Interestingly, the shape of the absorption spectrum for state II is virtually independent of θ, whereas that for state I is dependent on θ (compare Fig. 4 with Fig. 5; this was found to be true for the complete range of values for θ, results not shown).

The crucial question posed here is whether there is a criterion which we can use in order to choose an appropriate value (or a limited range of values) of θ for 7-methyl GMP. Such a choice must necessarily rely on the findings of studies of single-crystal polarized reflection[20,25] and linear dichroism from stretched films[26] for protonated guanine, 9-ethyl guanine and guanine. These studies have established that in the short-wavelength region state II is the predominantly absorbing state. By keeping in mind the above discussion (see also Appendix 1), we conclude that, for our results to be consistent with this premise, the resolution of the total absorption spectrum into the constituent absorption spectra for states I and II must be done in a manner which cannot be very different from that shown in Fig. 5. We note that in writing Eq. (2.5) we have assumed that the fast relaxation from state II to state I is a single-step process. If the relaxation process actually involves more than one step, then Eq. (2.5) generalizes to

$$r_b = 0.4P_2(< cos\alpha >) \times P_2(< cos\beta >) \times P_2(< cos\gamma >) \times P_2(< cos\delta >) \cdots \tag{2.9}$$

where $\alpha, \beta, \gamma, \delta$ are the angles subtended by the absorption transition dipole moments between these successive steps. The analysis above has, therefore, subsumed the product of the terms for $\beta, \gamma, \delta, etc.$ under one term which involves a single angle we called θ. In that case there is no straightforward relationship between this angle and the angle between the absorption transition dipole moments of states I and II. Such a con-

sideration may explain in part why the value for θ, which had to be used to satisfy the requirement that at the short-wavelength region the state that predominantly absorbs is state II, differs significantly from that obtained in the single-crystal[20,25] and stretched-film[26] studies.

It is seen from Fig. 5 that states I and II have spectral maxima at about 290 nm and 260 nm, respectively. These wavelengths are comparable to those reported in the crystal[20,25] and stretched film studies[26]. Absorption by state I predominates for wavelengths longer than about 295 nm, whereas absorption by state II predominates for wavelengths shorter than about 265 nm. An isosbestic point exists at about 285 nm. The absorption spectrum for state I appears to extend to about 260 nm. At shorter wavelengths, in addition to the absorption band for state II there is a weak band that has a maximum at about 245 nm. The increase in r in this spectral region (Fig. 1) implies that the polarization associated with the state responsible for this band is closer to that of state I than to state II. The energy spacing, however, makes it unlikely that this is a vibronic band of state I. There is considerable uncertainty regarding the shape of this band because of the fact that in this spectral region the exciting light intensity and the transmission of the excitation polarizer are low. These uncertainties notwithstanding, the present data suggest that this band makes a significant contribution to the total absorbance: its contribution at 244 nm is about 40%. We note that a weak band was reported by Clark[20] (1977) at about 227 nm for 9-ethylguanine and at about 215 nm for guanine hydrochloride from single-crystal polarized reflection measurements. Also, molecular orbital calculations by Hug and Tinoco[40] and Ito and I'Haya[39] predict a weak band at about 230 nm and 240 nm for 9-ethylguanine and guanine, respectively. Certainly, additional experimental and theoretical work is warranted in order to determine the origin of this band.

The values of the oscillator strength f can be calculated from the following equation[43]

$$f = 4.39 \times 10^{-9} \int \epsilon(\nu) d\nu \qquad (2.10)$$

where ν is the wavenumber and ϵ is the molar extinction coefficient. (We

obtained 1.16 x $10^4 M^{-1} cm^{-1}$ at 258 nm as the maximum value for ϵ.) We found them to be 0.11 and 0.21 for bands I and II, respectively. These values agree with those reported for the crystalline phase: 0.15 and 0.20 for guanine hydrochloride and 0.16 and 0.25 for 9-ethylguanine[20]. If the weak band centered at about 245 nm is considered to stem from another state (as is most likely the case), then its contribution may be estimated by graphical resolution of the band. (This resolution cannot be done by using equations analogous to those of 1 through 6 as the available information is insufficient.) In that case, the values of f for the weak band and for the band corresponding to state I are found to be about 0.04 and 0.07, respectively. Thus, the values of f for state I and state II are about 0.07 and 0.21, respectively.

Calculations of CD spectra for guanine-containing polynucleotides necessitate the resolution of the absorption spectrum of guanine into its component spectra. Such calculations[44,45], in which a graphical resolution of the spectra was employed, were unsuccessful in fitting the experimental CD spectra. It would certainly be of interest to carry out such calculations in which component spectra, obtained along the lines developed in the present study, are used. Of particular interest are the CD spectra of the left-handed helical conformation which poly(dG-dC)·poly(dG-dC) attains in the presence of high salt[46].

As can be seen from Fig. 5, both of the constituent absorption spectra exhibit some structure. A similar behavior for the spectrum of state I can be seen for 9-ethylguanine and guanine hydrochloride in the crystalline state[20]. The apparent energy spacings (Fig. 5) are somewhat larger than those usually associated with vibronic transitions; this suggests that there is an admixture of underlying vibronic bands whose resolution is obscured by the uncertainty associated with the data. This is in contrast to the absence of structure in the absorption spectra of all the other nucleotides[47], presumably because the broadenings of the vibronic levels are larger in those cases. (The fluorescence spectrum (Fig. 3) is seen to exhibit some structure as well.) The presence of structure may allow efficient migration of excitation energy between neighboring guanine residues in nucleic acids through resonance between individual

vibronic levels, the so-called weak interaction[48]. Such a mechanism for energy transfer in nucleic acids was previously suggested[49]. Its rate constant increases with the molar extinction coefficient, and this may serve as a test for its occurrence.

In the next chapter I discuss several aspects of energy transfer along the helix of a double-stranded nucleic acid.

Chapter 3

ENERGY TRANSFER IN METHYLATED DNA

Evidence for the involvement of transfer of electronic energy in the formation of photoproducts in double-stranded DNA comes from the observation that these photoproducts are clustered[50,51], rather than randomly distributed. Transfer of energy along the helix is of potentially great importance regarding photodamage in nucleic acids: this process may result in an increase in the probability that a base, which happens to be transiently open as a result of thermal fluctuations, may become excited and form a stable photoproduct[52].

We previously presented evidence that energy transfer takes place in calf thymus DNA which had 75% of its guanine residues methylated at position N-7[28]. Although methylation alters the B conformation somewhat, its double-strandedness is preserved[53,54].The methylated guanine bases are practically the only ones that are fluorescent and, in addition, absorb light at much longer wavelengths than the nonmethylated bases and, as a result, constitute an irreversible energy trap. These are very desirable properties which are not possessed by any of the bases of nonmethylated DNA.

In the present study we report the measurement of the efficiency of energy transfer from the other bases to the methylated guanines as a function of excitation wavelength. This is the first study that has accomplished such a measurement for transfer of energy along the DNA double helix. We also investigate the nature of the mechanism of transfer. We

have simulated the date by employing a stochastic model that uses the dipole-dipole term in the interaction potential for the coulombic interaction to calculate the rate constant of transfer[55]. Other terms are found to make only a small contribution to the overall efficiency of transfer. By comparison, the electron exchange mechanism of transfer[56]appears to be much less efficient.

3.1 Materials and Methods

Galf thymus DNA, highly polymerized, was obtained from Sigma Chemical Co (st. Louis, MO). Sodium cacodylate and sodium chloride were products of BDH Chemicals (Dorset, England) and Fisher Scientific Co. (Pittsburg, PA), respectively. Dimethyl sulfate was obtained from Aldrich Chemical Co. (Milwaukee, WI). Membrane cleaning agents for DNA methylation were supplied by Spectrum Medical Industries (Los Angeles, CA).

Methylatiln of calf thymus DNA at the N-7 position of the guanine residue was carried out according to the method of Ramstein et al.[53]. To a 4 ml DNA solution (1 mg/ml in 0.5 M sodium cacodylate, 1 M NaCl, pH 6.6 prepared in triply distilled water) at 0°C, 70 μl of dimethyl sulfate were added every 30 min. for 3 h. The product was dialyzed at 0°C against the same buffer for 1 h and then against 0.05 M sodium cacodylate, 0.01 M NaCl, pH 6.6, for a further 3 h. The dialysis membrane used in this process was prewashed from sulfur and heavy metals. Aliquots of methylated DNA solution were kept at -20°C and used within 1 week.

The degree of guanine methylation, determined by comparing the melting temperature of methylated DNA with that of DNA[53], was found to be about 75%. The only fluorescent product of methylation is 7-methyl guanine[28,53,57].

Fluorescence spectra were taken with a spectrofluorometer previously described at Chapter 2. The spectra were corrected for the variation of the sensitivity of the photomultiplier-monochromator combination with emission wavelength by employing a standard lamp[29]. The excitation and emission bandwidths were 1.7 and 5 nm, respectively.

Fluorescence quantum yields were determined by comparing the areas under the fluorescence spectra with that of a p-terphenyl solution in cyclohexane and were corrected for the difference in refractive indices of water and cyclohexane[43].

The buffer used for all solutions consisted of 0.05 M sodium cacodylate, 0.01 M NaCl, pH 6.6 (in triply distilled water). The absorbance of the samples at 260 nm was about 0.05. All measurements were carried out at room temperature. A correction was made for buffer contribution to emission.

3.2 Calculations of Transition Dipole Moments

Two mechanisms for energy transfer may operate: (i) the coulombic and (ii) the electron exchange. Förster[55] formulated a theory for (i) based on the dipole-dipole term in the interaction potential in which the rate constant varies as R^{-6}, where R is the donor-acceptor distance. Dexter[56] formulated a theory for mechanism (ii) in which the rate constant decreases exponentially with R. Unlike Förster's theory, however, Dexter's theory contains a parameter that cannot be obtained from the optical properties of the donor and the acceptor. Below, we test how well Förster's theory describes the experimental data. (An approximate comparison is also made with Dexter's theory.)

According to the dipole-dipole mechanism of transfer, the critical transfer distance, R_o, is defined as the donor-acceptor distance at which the rate of transfer is equal to the decay rate of the donor in the absence of energy transfer. R_o is given by

$$R_o^6 = \frac{8.79 \times 10^{-25} k^2 \phi_0}{n^4} \int_0^\infty \frac{F(\bar{\nu})\epsilon(\bar{\nu})d\bar{\nu}}{\bar{\nu}^4} \qquad (3.1)$$

In Equation (3.1), n is the refractive index of the medium between the bases ($n \approx 1$), ϕ_0 is the fluorescence quantum yield of the donor in the absence of an acceptor, k is an orientational factor (see below Equation (3.2)), $\epsilon(\bar{\nu})$ is the molar extinction coefficient of the acceptor at wavenumber $\bar{\nu}$, and $F(\bar{\nu})$ is the fluorescence intensity of the donor at $\bar{\nu}$

(with the fluorescence spectrum normalized to unity on a wavenumber scale). Below, we will use the symbol J to denote the spectral overlap in Equation (3.1).

The values of k (Appendix II) were calculated from

$$k = [\mathbf{u_d} \cdot \mathbf{u_a} - 3\frac{(\mathbf{u_d} \cdot \mathbf{R})(\mathbf{u_a} \cdot \mathbf{R})}{\mathbf{R^2}}]/|\mathbf{u_d}| \cdot |\mathbf{u_a}| \qquad (3.2)$$

In Equation (3.2) $\mathbf{u_d}$ and $\mathbf{u_a}$ are the transition dipole moments of the donor and the acceptor, respectively, and R is the center-to-centr donor-acceptor distance (Appendix II). The directions of the transition dipole moments were obtained from the literature[2,15,20,25,26]. For guanine, we used the transition dipole moment of the lower-energy state because we found that the upper-energy state does not fluoresce but converts to the lower one with 100% efficiency. We have also done this for adenine[15].

In the calculations we have used the fluorescence[21] and absorption[47,58,59] spectra of free nucleotides. It was reported [53] that in methylated DNA about 20% of the A bases are methylated at position 3. In our calculations we did not take into account the presence of 3-methyl A. It was felt that this omission will not introduce a relatively large error in the analysis of the data. It should be noted that 3-methyl A does not fluoresce[57]. Approximate hypochromicity and hyperchromicity corrections for the latter in the 240-290 and 295-305 nm spectral regions, respectively, were made as described in the literature[60–63]. The values for J are listed in Appendix III. We note that we have found the value for J to be very small for transfer from methylated guanine to any of the A, T, C or G bases. Thus, the former base is in effect an irreversible energy trap.

3.3 Results and Discussion

We have measured the apparent fluorescence quantum yield, Q, of methylated DNA as a function of excitation wavelength (Figure 6). At 305 nm the fluorescence quantum yield, q=6.7×10^{-4}, of the methylated guanine bases is obtained, as at this excitation wavelength the fraction of the exciting light absorbed by the other bases is virtually negligible.

Also plotted in Figure 6 is the product αq, where α is the fraction of light absorbed by the methylated guanine residues. It is seen that, for all excitation wavelengths, Q is much larger than this product. We attribute this difference to transfer of some of the photons absorbed by the other bases to the methylated guanine bases which constitute an (irreversible see below) energy trap. Thus, we express Q as follows:

$$Q = q\alpha + (1 - \alpha)qf \tag{3.3}$$

Here, the first term represents direct absorption of light by the trap, whereas the second term represents transfer of energy to it from the other bases with an overall efficiency f. We consider q to be independent of the excitation wavelength, in view of our previous finding that the fluorescence quantum yield of 7-methyl GMP is independent of the excitation wavelength.

Figure 7 plots the values of f, obtained through Equation (3.3), as a function of excitation wavelength. It is seen that f increases as the excitation wavelength is increased. On the average, about one out of every three photons absorbed by the other bases is transferred to the trap. In Equation (3.3) all of the observed fluorescence is attributed to the trap. This overestimates the experimental values of f. It can be easily shown that, if q′ is the apparent fluorescence quantum yield of the energy-donating bases in the absence of energy transfer to the trap, Equation(3.3) is modified as follows

$$Q = \alpha q + (1 - \alpha)[q' + (q - q')f] \tag{3.4}$$

By using $q' = 3 \times 10^{-5}$ (the reported fluorescence quantum yield of DNA,see below), we find from Eqution (3.4) that, on the average, f is reduced by $\approx$ 10% relative to that obtained from Equation (3.3) that assumes $q\prime = 0$ (Figure 7).

We have used a stochastic model for energy transfer along the helix of methylated DNA in order to estimate the efficiency with which the excitation energy is trapped. In this model energy transfer is treated as a random walk among adjacent bases. The parameters of the model are the relaxation rate constants k_i of a nonmethylated base of type i (i =

1, 2, 3 and 4 for G, C, T, and A, respectively) in the absence of energy transfer, and the rate constants of energy transfer k_{ij}^u and k_{ij}^d between a base of type i and an adjacent base of type j going from 3′ to 5′ or 5′ to 3′ , i.e., for the two possible geometries between adjacent bases on the same strand (j = 0 is used to denote a methylated base). The rate constants k_{ij}^u and k_{ij}^d are of the form $k_i(R_0/R)^6$ [55]. The probability that energy transfer will occur along a given path can be calculated directly from the ratio of th rate constants k_{ij}^u or k_{ij}^d and k_i. This ratio is proportional to R_0^6 which, in turn, is proportional to the fluorescence quantum yield ϕ_0 in the absence of energy transfer to the trap (see Equation (3.1)). Thus, these calculations do not necessitate a knowledge of the relaxation rate constants k_i. For the range of values considered for the various rate constants, we found that transfer paths of more than four steps had a total probability of about one per cent; the first step made a contribution of about 85% to the overall efficiency of transter. Consequently, for intrastrand transfer, it was possible to limit calculations of trapping efficiency to the classes of energy transfer paths depicted in Figure 8. We consider only transfer between nearest neighbors. For transfer between next nearest neighbors, the distances are much larger, which makes the transfer inefficient because of the strong dependece of the rate constant of transfer on distance. For C hydrogen bonded to the trap, despite the large distande (about 7.3 Å), interstrand transfer make a significant contribution (see below). Consequently, we have included this transfer path in the simulations (Figure 8); because two-step transfer was found to make a contribution of only about 5% to the overall transfer efficiency, more steps were omitted. We omitted interstrand transfer between C and G because: (i) only 25% of the Gs are nonmethylated; and (ii) for energy trapping to occur through this path at least one additional step is required, for which case we found the efficiency to be low (see below). When A is the donor or the acceptor, the data analysis finds that transfer is inefficient. The model follows.

The probabilities $p_{i_0mn}^d$ and $p_{i_0mn}^b$ that excitation of a base of type i_0 will be followed by transfer through m steps and n bases to a trap (i.e., to a base of type $i_n = 0$) from 5′ to 3′ and interstrand transfer are given

by the formulas

$$p^d_{i_0 11} = q_0 \sum_{i_{-1}=0}^{4} q_{i_{-1}} \sum_{i_{b_1}=0}^{1} \frac{q_{i_{b_1}}}{q_0+q_1} \frac{k^d_{i_0 0}}{k^d_{i_0 0} + k^u_{i_0 i_{-1}} + k_{i_0} + k^{b_1}_{i_0 i_{b_1}} \delta_{i_0 2}} \tag{3.5}$$

$$p^{b_1}_{i_0 11} = \frac{3}{4} \sum_{i_1=0}^{4} q_{i_1} \sum_{i_{-1}=0}^{4} q_{i_{-1}} \frac{k^{b_1}_{i_0 0} \delta_{i_0 2}}{k^{b_1}_{i_0 0} + k^u_{i_0 i_{-1}} + k^d_{i_0 i_1} + k_{i_0}} \tag{3.6}$$

$$p^d_{i_0 22} = q_0 \sum_{i_{-1}=0}^{4} q_{i_{-1}} \sum_{i_1=1}^{4} q_{i_1} \sum_{i_{b_1}=0}^{1} \frac{q_{i_{b_1}}}{q_0+q_1} \sum_{i_{b_2}=0}^{1} \frac{q_{i_{b_2}}}{q_0+q_1} \cdot$$
$$\cdot \frac{k^d_{i_0 i_1}}{k^d_{i_0 i_1} + k^u_{i_0 i_{-1}} + k_{i_0} + k^{b_1}_{i_0 i_{b_1}} \delta_{i_0 2}} \frac{k^d_{i_1 0}}{k^d_{i_1 0} + k^u_{i_1 i_0} + k_{i_0} + k^{b_2}_{i_1 i_{b_2}} \delta_{i_1 2}} \tag{3.7}$$

$$p^b_{i_0 22} = \frac{3}{4} \sum_{i_{-1}=0}^{4} q_{i_{-1}} \sum_{i_1=1}^{4} q_{i_1} \sum_{i_2=0}^{4} q_{i_2} \sum_{i_{b_1}=0}^{1} \frac{q_{i_{b_1}}}{q_0+q_1} \cdot$$
$$\cdot \frac{k^d_{i_0 i_1}}{k^d_{i_0 i_1} + k^u_{i_0 i_{-1}} + k_{i_0} + k^{b_1}_{i_0 i_{b_1}} \delta_{i_0 2}} \frac{k^{b_2}_{i_1 0} \delta_{i_1 2}}{k^{b_2}_{i_1 0} + k^u_{i_1 i_0} + k^d_{i_1 i_2} + k_{i_0}} \tag{3.8}$$

$$p^d_{i_0 33} = q_0 \sum_{i_{-1}=0}^{4} q_{i_{-1}} \sum_{i_1=1}^{4} q_{i_1} \sum_{i_2=1}^{4} q_{i_2} \frac{k^d_{i_0 i_1}}{k^d_{i_0 i_1} + k^u_{i_0 i_{-1}} + k_{i_0}} \cdot$$
$$\cdot \frac{k^d_{i_1 i_2} k^d_{i_2 0}}{(k^d_{i_1 i_2} + k^u_{i_1 i_0} + k_{i_1})(k^d_{i_2 0} + k^u_{i_2 i_1} + k_{i_2})} \tag{3.9}$$

$$p^d_{i_0 31} = q_0 \sum_{i_{-1}=1}^{4} q_{i_{-1}} \sum_{i_{-2}=0}^{4} q_{i_{-2}} \frac{k^u_{i_0 i_{-1}}}{k^u_{i_0 i_{-1}} + k^d_{i_0 i_1} + k_{i_0}} \cdot$$
$$\cdot \frac{k^d_{i_{-1} i_0} k^d_{i_0 0}}{(k^d_{i_{-1} i_0} + k^u_{i_{-1} i_{-2}} + k_{i_{-1}})(k^d_{i_0 0} + k^u_{i_0 i_{-1}} + k_{i_0})} \tag{3.10}$$

$$p^d_{i_0 44} = q_0 \sum_{i_{-1}=0}^{4} q_{i_{-1}} \sum_{i_1=1}^{4} q_{i_1} \sum_{i_2=1}^{4} q_{i_2} \sum_{i_3=1}^{4} q_{i_3} \frac{k^d_{i_0 i_1} k^d_{i_1 i_2}}{(k^d_{i_0 i_1} + k^u_{i_0 i_{-1}} + k_{i_0})(k^d_{i_1 i_2} + k^u_{i_1 i_0} + k_{i_1})} \cdot$$
$$\cdot \frac{k^d_{i_2 i_3} k^d_{i_3 0}}{(k^d_{i_2 i_3} + k^u_{i_2 i_1} + k_{i_2})(k^d_{i_3 0} + k^u_{i_3 i_2} + k_{i_3})} \tag{3.11}$$

$$p^d_{i_0 42} = q_0 \sum_{i_1=1}^{4} q_{i_1} [\sum_{i_{-1}=0}^{4} q_{i_{-1}} (\frac{k^d_{i_0 i_1}}{k^d_{i_0 i_1} + k^u_{i_0 i_{-1}} + k_{i_0}})^2 \cdot$$

$$\cdot \frac{k^u_{i_1 i_0} k^d_{i_1 0}}{(k^u_{i_1 i_0} + k^d_{i_1 i_0} + k_{i_1})(k^d_{i_1 0} + k^u_{i_1 i_0} + k_{i_1})} +$$

$$+ \sum_{i_{-1}=1}^{4} q_{i_{-1}} \sum_{i_{-2}=0}^{4} q_{i_{-2}} \frac{k^u_{i_0 i_{-1}} k^d_{i_{-1} i_0}}{(k^u_{i_0 i_{-1}} + k^d_{i_0 i_1} + k_{i_0})(k^d_{i_{-1} i_0} + k^u_{i_{-1} i_{-2}} + k_{i_{-1}})} \cdot$$

$$\cdot \frac{k^d_{i_0 i_1} k^d_{i_1 0}}{(k^d_{i_0 i_1} + k^u_{i_0 i_{-1}} + k_{i_0})(k^d_{i_1 0} + k^u_{i_1 i_0} + k_{i_1})}]. \qquad (3.12)$$

In these equations, δ is the Kronecker delta, q_i is the fraction of bases of type i, the superscript b denotes interstrand transfer from C and i_b designates a base hydrogen bonded to a C. Substitution of the superscript d by u and vice versa yields the corresponding formulas for transfer from $3'$ to $5'$. The efficiency with which light exciting bases of type i is trapped is

$$p_i = \sum_{m=1}^{\infty} p^d_{i,m} + p^u_{i,m} + p^b_{i,m} \delta_{i2} \delta_{m1} + p^b_{i,m} \delta_{i2} \delta_{m2} \qquad (3.13)$$

The overall trapping efficiency for excitation at wavelength λ_{ex} is then

$$f_{\lambda_{ex}} = \sum_{i=1}^{4} a_i(\lambda_{ex}) p_i / \sum_{i=1}^{4} a_i(\lambda_{ex}) \qquad (3.14)$$

where $a_i(\lambda_{ex})$ is the absorbance of the bases of type i at λ_{ex}.

There is no information regarding the individual values of the fluorescence quantum yield ϕ_0 for the A, T, C and G bases in the absence of transfer to the trap. In principle, one can obtain an average value for ϕ_0 from $\phi_0 = \tau_0/\tau_{rad}$, whewe τ_0 is the fluorescence lifetime of DNA and $\tau_{rad} \approx 5$ ns[4,64] is the radiative lifetime of the DNA bases. Two measurements of τ_0 have been reported. Values of about 10 ps and 65 ps were reported[34] in the short- and long-wavelength spectral regions, respectibely, by using a picosecond streak camera. Another study[65] used singl-photon detection and obtained in the short-wavelength spectral region a value of about 3 ns, which made a contribution of about 20%, but could not resolve the remaining fast components. Thus, the uncertainty

in the values of the fluorescence decay components precludes an estimate of ϕ_0.

A potentially useful approach to draw inferences regarding the ability of the different bases to fluoresce is the following. It is known from low- and room-temperature measurements[6,21] that the polynucleotide poly(dA-dT)·poly(dA-dT) fluoresces rather well. The polynucleotide poly(dG-dC)·poly(dG-dC), however, was reported not to fluoresce appreciably at low temperature[6]. Our preliminary measurements show that at room temperature and for excitation at 265 nm this polynucleotide fluoresces much less strongly than does poly(dA-dT)·poly(dA-dT) (Huang, Ge, and Georghiou, to be published). These results appear to suggest that in DNA fluorescence stems from the A-T base pairs. This inference, however, is questionable on the following grounds: (i) fluorescence from poly(dA-dT)·poly(dA-dT) involves excimers (ref. 21 and Ge and Georghiou, to be published), whereas the contribution of excimer emision to the fluorescence spectrum of random-sequence DNA does not appear to be very large[21,66]; and (ii) although both of these polynucleotides appear to have a B-type conformation in solution[67–69], they allow only (A,T) or (G,C) base stacking interactions and no other types of such interactions which do occur in random-sequence DMA.

In view of the absence of a direct method to obtain approximate values for ϕ_0, we are forced to rely on other, more indirect methods. Examination of Figure 7 shows that the experimental values of the efficiency f of energy transfer to the trap are quite low in the short- wavelength region in which the fraction of light α_A absorbed by A is quite high: e.g., at 260 nm, f = 0.22 and $\alpha_A \approx 0.41$, whereas at 290 nm, f = 0.42 and $\alpha_A \approx 1\%$. This suggests that A is a very poor energy donor. The efficiency f' for one-step pairwise transfer is given by[55]

$$\frac{1}{f'} = 1 + (\frac{R}{R_0})^6 = 1 + k_{ij}^2 \tag{3.15}$$

By combining Equations (3.5) and (3.1), we have

$$\frac{1}{f'} = 1 + \frac{R^6}{8.79 \times 10^{-25} n^{-4} k^2 J \phi_0} \tag{3.16}$$

It is seen from Equation (3.15) that the efficiency f' increases as J, k^2 and ϕ_0 increase. For transfer from A, the values of J are larger than those when the other bases are the donors (Appendix III). On the other hand, the value of k^2 for A-trap transfer is very small (Appendix II). As the simulations show (see below), the range of the transfer process along the helix is rather limited, and, therefore, base-trap transfer makes a very significant contribution to the overall transfer efficiency f. Consequently, the small value of k^2 for adjacent A-trap transfer is an important cause of the observed reduction in f at short excitation wavelengths (Figure 7). In addition, however, the simulations require that the value of ϕ_0 for A be very small. In Appendix IV we list the simulated f values obtained for different combinations of ϕ_0 values for the bases. It is seen that, when the value of ϕ_0 for A as well as those for T, C, and G are equal to 3×10^{-4}, the simulated values of f are not very different from the experimental ones in the short-wavelength region but are much lower in the long-wavelength region. This implies that the latter ϕ_0 value should be increased whereas the former should be decreased. Indeed, the combination that results in the most satisfactory fit is ϕ_0 for A in the 10^{-6} to 10^{-5} range and ϕ_0 of about 2×10^{-3} for T, C, and G (Appendix IV). It is also of interest to note is this regard that A does not from a significant number of photoproducts in DNA[70,71], whereas T and C do[72]. This is consistent with the notion that A does not fluoresce significantly, whereas T and C do: a significant value for the fluorescence quantum yield implies a decay time which is significantly long, one during which T or C could undergo excited-state reactions that might lead to the formation of photoproducts. In view of these considerations, we have considered the fluorescence quantum yield ϕ_0 of A to be very small and have let those of T and C be equal to each other. Two recent reports[73,74], ascribe a high degree of forbiddeness to the lowest excited singlet state of uracil and adenine, with the value of the radiative rate constant, k_f, being very small. It should be noted that in principle this would not preclude transfer of energy from A, as f' depends on ϕ_0, not k_f (see Equation (3.15) and Ref. 75). There is no information regarding photoproduct formation by G. In our calculations we have let the quantum yield of G (which bases constitute only about 5% of the

total DNA bases) be equal to those of T and C. (For a quantum yield of G equal to 1×10^{-6}, we found the efficiency of transfer, obtained through the stochastic model, to decrease by about 5% across the excitation spectral range.)

As was stated above, the stochastic model finds that a value of about 2×10^{-3} is needed for ϕ_0 of T, C, and G in order to obtain values of f which are comparable to the experimental ones (Figure 7). The average number of steps the excitation energy takes to reach the trap is found to be about 1.2 and is independent of the excitation wavelength; that is to say, energy transfer in effect requires that the donating base be a nearest or next nearest neighbor of the trap. (By contrast, it has been estimated[52] that triplet-triplet energy transfer might have a range of $10^3 - 10^4$ bases.) As seen from Appendixs II and V, the R_0/R values are quite large (about 1.5) for base-trap transfer so that, on the average, they yield from Equation (3.15) a value of about 0.93 for the efficiency f' for one-step transfer. The f' vs. R_0/R plot (not show) is close to being flat for these large R_0/R values. Also, the simulations with the stochastic model show that the increase in f that results from an increase in ϕ_0 beyond 2×10^{-3} is very small (see Appendix IV). Consequently, the value of ϕ_0 for T, C, and G necessary to approximate the experimental results, although it cannot be accurately determined, is not very different from 2×10^{-3}. An estimate of the average value for the fluorescence decay time of DNA for monomeric emission implied by $\phi_0 \approx 2 \times 10^{-3}$ can be obtained from $\tau_0 = \phi_0\tau_{rad} \approx 2\times10^{-3}\times5\times10^{-9}s \approx 10ps$. As was discussed above, a value of about 10 ps was reported[34] for the short-wavelength spectral region, but the possibility remains that other decay components may be present with decay times shorter than ≈3 ps or in the nanoseconed time range which could not be detected in that study; in this regard, a 3-ns decay component was reported for the short-wavelength spectral region[65]. This value is about two orders of magnitude higher than that of about 3×10^{-5} reported for DNA[21,66,76,77]. Thus, according to the results of these simulations, the transfer process between adjacent bases takes place from their excited electronic states before a very efficient quenching process sets in: formation of excited-state molecular comoplexes (excimers), that

do not fluoresce appreciably, could account for these observations. The contribution of excimer emission to the fluorescence spectrum of DNA does not appear to be very large[21,66]. the fluorescence spectrum peaks at about 330 nm and is consistent with emission stemming from a rather small fraction of excited bases that do not participate in excited-state complex formation; there is also a long-wavelength shoulder which is consistent with some emission stemming from such complexes[66].

The major driving forces for excimer formation stem from exciton-resonance and charge-resonance interactions. The most stable configuration is that of a sandwich in which the two molecular planes are parallel to each other and overlap either partially or completely. Other configurations, however, have also been considered in which one of the molecules is rotated relative to the other, such as those for naphthalene[78] and benzene[43]. The occurrence of such configurations has been inferred for intramolecular excimers in some systems in which the two partners are linked together with an aliphatic chain[79–81]: the conformation necessary for the sandwich excimer would be highly strained in those particular systems. (The nonsandwich excimers tend to be stabilized by charge-resonance interactions, whereas the exciton-resonance interaction is mainly responsible for the stability of the sandwich excimer[43].) Although some displacement may be necessary for achieving the optimum molecular overlap, the interplanar distance of 3.4 Å between adjacent DNA bases is in fact very similar to that encountered in a typical aromatic excimer (about 3.3 Å, Ref. 43). These considerations suggest that a nonsandwich excimer might be formed in DNA. A sandwich excimer, however, would necessitate both base displacement as well as rotation; these motions might be defficult to achieve because of the rather short lifetime of the excited DNA bases and because of the distortion of the DNA helix which they would introduce. It is also probable that in the ground electronic state some of the bases are held loosely together in a geometry which favors excimer formation. (It should be pointed out that there is no strong ground-state interaction between the bases, as no pronounced changes in the vibronic envelope of the absorption spectrum of DNA are observed relative to that of an equivalent molar mixture of

monomers.) Information on the formation of excimers is of particular importance regarding photodamage of DNA because of their potential involvement as precursors in the formation of photoproducts[6].

The rate constant for intrastrand transfer between adjacent bases is estimated from $(\phi_0\tau_{rad})^{-1}(R_0/R)^6$ (see Ref. 55) to be about 2×10^{11} s^{-1} based on average values of 4.3 Å for R_0 form Appendix V and 4.0 Å for R from Appendix II, and about 5ns for τ_{rad} [4,64]. On the other hand, the rate constant for base-trap transfer is found to be larger, about 1×10^{12} s^{-1} for an average value of 6.3 Å for R_0 (Appendix V). The quastion arises as to whether this rate is faster than the rate of vibronic relaxation. The value for the latter is not accurately known but or expected to be in the range of 10^{12} to 10^{13} s^{-1}. Interestingly, it appears that vibronic relaxation in the free bases takes place on the subpicosecond time scale[31]. As we point out below, the fact that we did not observe an increase in the efficiency of transfer when exciting in the short-wavelength spectral region (Figure 7) argues against the occurrence of before-relaxation transfer in the present system. For interstrand transfer, only C-trap transfer makes a significant contribution. In that case, $R \approx 7.3$ Å, $k^2 \approx 1.3$ and $R_0 \approx 9$ Å (from Equation (3.1)), which yield a value of about 4×10^{11} s^{-1} for the rate constant for transfer. The efficiency of this transfer is found from Equation (3.16) to be about 0.78. This value is to be compared with those of 0.93 and 0.61 for intrastrand base-trap and base-base transfer, respectively. Tramsfer that involves A either as a donor or an acceptor is inefficient.

We now examine the validity of the dipole-dipole mechanism of energy transfer for the present system. For the coulombic mechanism, the interaction potential is expanded as a series of inverse power of the intermolecular distance R. For distances that are large compared to molecular dimensions, the dipole-dipole term, that varies as R^{-3}, predominates. This is not strictly valid for the present system. The other two leading terms are the dipole-quadrupole and the quadrupole-quadrupole that vary as R^{-4} and R^{-5}, respectively. Dexter[56] estimates that the ratio of the dipole-quadrupole rate constant to that of the dipole-dipole is of the order of $(\beta/R)^2$, where β is the molecular radius. For the bases,

$\beta \approx 3$ Å[84]. Thus, for $R \approx 4$ Å (Appendix II), the dipole-quadrupole term appears to be making a contribution to the rate constant of intrastrand transfer of ~50% relative to that made by the dipole-dipole term. For one-step transfer, this would require that $\phi_0 \approx 1 \times 10^{-3}$, instead of $\phi_0 \approx 2 \times 10^{-3}$ for the dipole-dipole term alone (see Equation (3.16)). But as was pointed out above,the f' vs. R_0/R plot is almost flat for the present R_0 and R values (Appendixs II and V); consequently, it is found that this will change f by only about 10% (see Appendix IV). (This is only an approximate result, of course, since the stochastic model finds that the average number of steps in the transfer process for this case is about 1.2, not 1 as we assumed in obtaining $\phi_0 \approx 1 \times 10^{-3}$.) From the calculations of Förster[83] we find that the quadrupole-quadrupole term does not appear to be making a large contribution for the distances involved in the present system. Such a conclusion is also reached from the calculations of Voltz[84] regarding the dipole-octupole and the octupole-octupole terms. For C-trap interstrand transfer, the distance is much larger (about 7.3 Å) than that for intrastrand transfer; as a result, the contribution of these terms is even smaller.

Förster's mechanism involves the so-called very weak interaction. The other two interactions are the weak and the strong[55]. The latter does not operate for DNA as no pronounced changes in the vibronic envelope of its absorption spectrum are observed relative to that of an equivalent molar mixture of monomers. The weak interaction involves resonances between individual vibronic levels and, therefore, does not apply to systems that do not exhibit vibronic structure in their absorption spectra[55]; this is the case for the spectra of T, A and C. Guanine is an exception to this. Its long-wavelength absorption spectrum contains two bands[20,25,26]. We have recently shown that, resolution of the spectrum into those corresponding to the two electronic transitions which are present, reveals the presence of vibronic structure. That work employed 7-methyl guanosine 5′-phosphate. It was argued there that the conclusions drawn most probably apply to the nonmethylated nucleotide as well. Thus, transfer of energy can possibly occur between individual vibronic levels in guanine. (This could also happen between two adjacent traps but this would

not affect the overall efficiency of base-trap transfer.) Since according to this mechanism the rate constant of transfer is proportional to the molar extinction coefficient[83,85], one would expect to observe an enhancement of f at about 260, 275 and 290 nm which are the maxima of the vibronic bands. This is not observed. In any case, the nonmethylated G bases are only about 25% of all the G bases in methylated DNA and, therefore, G-G sequences are not frequent. Another possibility is transfer before vibronic relaxation by the very weak interaction[64]. In that case, however, f is expected to increase for excitation in the short-wavelength spectral region. The trend observed for f is contrary to this prediction (Figure 7). It could be argued that, in the short-wavelength excitation region, energy transfer may take place from the second excited state (state II) of the trap to an adjacent base before relaxation to the first excited state (state I) of the trap, which is the emitting state. We have found the absorption spectra for these states to overlap one another considerably. Thus, very few vibrational levels of state I are isoenergetic with state II, and, as a result, the rate of relaxation of state II to state I is expected to be reduced[86,87]. In this regard, our preliminary study of energy transfer in poly(dG-dC)·poly(dG-dC) (Huang and Georghiou, to be published) suggests that this type of transfer takes place from G to C. The values of the efficiency of intra- and interstrand basetrap transfer for the present system, however, are about 90% and 80%, respectively (see above); consequently, the accepting base will transfer the energy back to the trap rather efficiently. Thus, trap-base transfer, although it could make some contribution, is not expected to account for the large drop (about 300%, see Figure 7) of the experimemtal value of f upon going from 295 to 255 nm. Instead, the bulk of this drop appears to stem mainly from a very low value of ϕ_{0A}. Even a small value, 1×10^{-4}, for ϕ_{0A} is found to result in an increase of about 50% in the simulated value of f at 260 nm, from 0.23 (when $\phi_{0A} = 1 \times 10^{-6}$) to 0.34. ($\phi_{0T,C,G}$ was kept equal to 2×10^{-3} in this comparison.)

An alternative mechanism is that of electron exchange[87], which may operate for the short donor-acceptor distances involved in nucleic acids. According to this mechanism, the rate constant of transfer is, in effect,

independent of ϕ_0[56,88]. This property makes this mechanism potentially attractive for nucleic acids because of their very low fluorescence quantum yield. The expression for the rate constant of transfer, however, contains a parameter that cannot be determined from the optical properties of the donor-acceptor pair. This prevents detailed modelling. An approximate comparison with the dipole-dipole mechanism can be made, however, by using the value of 20 cm^{-1}, which was calculated[89] for the exchange energy, U, in polydA. (This value is very similar to those reported for adjacent aromatic molecules in crystals[90,91].) The rate constant of transfer w is given by[10]

$$w = \frac{4\pi^2 U^2 J}{h} \tag{3.17}$$

Where h is Planck's constant and J is the overlap between the fluorescence spectrum of the donor and the absorption spectrum of the acceptor. (Note that both spectra are normalized to unity on an energy scale.) We found the average value of J for base-base transfer to be about 6×10^{-7} cm. From Equation (3.17) we then obtain $w \approx 3 \times 10^8$ s^{-1}. On the other hand, for the dipole-dipole mechanism we found the rate constant for base-base transfer to be about 2×10^{11} s^{-1} (see above). Even if we consider a reduction in R, e.g. from 4 to 3 Å, the exponential dependence of U^2 on R^{12} would result in $w \approx 1 \times 10^9$ s^{-1} for the exchange interaction, which is still very small. Also, for C-trap interstrand transfer w will be very small because R$\approx$ 7.3 Å. Thus, electron exchange appears to be very inefficient as compared to the dipole-dipole mechanism of transfer.

3.4 Conclusion

We briefly examine the assumptions that were found necessary in the analysis of the data. We have used the absorption spectra of free nucleotides, but applied approximate hypo- and hyperchromicity corrections. This should not introduce a large uncertainty in the values of f. For example, increasing the fraction of light α absorbed by the trap by 10% at 265 nm is found to result in a decrease in f by only about 4%. The simulations require that the value of ϕ_0 (i) for C, T, and G be about 2×10^{-3}

and (ii) for A be very small. As was discussed above, the absence of a significant number of photoproducts formed by A in DNA is consistent with (ii). As for (i), it suggests transfer of energy before the fluorescence is quenched very efficiently, presumably by excimer formation. In this regard, the fluorescence spectrum of DNA[67] exhibits a long-wavelength shoulder which is consistent with some emission stemming from excimers. Its short-wavelength region, however, was reported to virtually coincide with that of an equimolar mixture of mononucleotides[67]. This implies that using the flourescence spectra of the latter in the calculation of the spectral overlap J with the absoption spectra of the energy-accepting bases should not introduce a serious error in the analysis of the data. (It shoud be noted in this regard that no excimer emission is detected from the methylated guanine residues of metylated [4,28,53].) In the simulations we used Förster's theory to calculate the rate constant of transfer. This uses only the dipole-dipole term in the expansion of the interaction potential. As was discussed above, incluaion of the dipole-quadrupole term, which is the only additional term that makes a significant contribution to the rate constant of transfer, should not have a large effect on f. The value of the refractive index n was taken to be equal to about 1, since, for transfer between nearest neighbors, no medium intervenes between donors and acceptors. Finally, the simulations assume that the bases are randomly distributed. If the frequency of the A-trap sequence is reduced, then the simulated value of f will increase because A turns out to be a very poor energy donor. This as well as other aspects of the transfer process will be investigated by using oligonucleotides of known sequence.

In summary, we have presented the first experimental determination of the efficiency of transfer of electronic energy along the helix of a double-stranded nucleic acid. This determination became possible by methylating about 75% of the Gs at the N-7 position. This resulted in the formation of an irreversible energy trap which essentially is the only fluorescent base in methylated DNA. About one out of every three photons absorbed by the other bases is trapped. Simulations in the framework of the coulombic interaction yielded for intrastrand base-base and base-

trap transfer values for R_0/R of about 1.1 and 1.5, respectively. For C-trap interstrand transfer (the only interstrand transfer that makes a significant contribution), it is found that $R_0/R \approx 1.2$. The corresponding values of the efficiency of pairwise transfer are about 60%, 90%,and 80%. Transfer is inefficient when A is the donor or the acceptor. The simulations require that the value of the fluorescence quantum yield of A be very small, whereas that of C, T, and G be about 2×10^{-3}. This value is much larger than the measured valur of the fluorescence quantum yield of DNA, about 3×10^{-5}. Thus transfer of energy precedes a process which results in a very efficient quenching of the fluorescence of DNA. Formation of excimers could be responsible for this effect. In this regard, the fluorescence spectrum of DNA[67] exhibits a shoulder at long wavelengths which appears to have its origin in emission from excimers.

As for nonmethylated DNA, the present results imply that intrastrand base-base transfer occurs with an efficiency of about 60%. Interstrand transfer betwee C and G occurs with an efficiency of about 35%; this calculation is based on the values $R \approx 7.3$ Å, $k^2 \approx 1.3$ and $R_0 \approx 5 \times (1.3/0.26)^{1/6} \approx 6.5$ Å (see also Appendixs III and IV). (For methylated DNA this latter transfer dose not make a significant contribution to the overall tramsfer efficiency because (i) only about 25% of the Gs are nonmethylated and (ii) in order for a photon to reach the trap through this path at least one additional step is required, for which case we fond the efficicncy of energy trapping to be low.) For both types of transfer the range is short because the excited states decay quite rapidly. Also, when A is the donor or the acceptor, the efficiency is very low.

REFERENCES

1. Watson, J. D. and F. H. C. Crick (1953) Nature, **171**, 737.

2. Callis, P. R. (1983) Ann. Rev. Phys. Chem., **34**, 329.

3. Vigny, p. and M. Duqesne (1976) In Organic Molecular Photchem. **3**, 167.

4. Deniels, M. and W. W. Hauswirth (1971) Science **171**, 675.

5. Deniels, M. and W. W. Hauswirth (1971) Photochem. Photobiol. **13**, 157.

6. Gueron, M., J. Eisinger and A. A. Lamola (1974) In Basic Principles in Nucleic Acid Chemistry, Vol 1, P. O. P. Ts'o, Academic Press, NY.

7. Murrell, J. N. (1963) The Theory of Electronic Spectra of Organic Molecules, 125.

8. Callis, P. R., T. W. Scott and A. C. Albrecht (1983) J. Chem. Phys., **78**, 16

9. Scott, T. W., P. R. Callis and A. C. Albrecht (1982) Chem. Phys. Lett., **93**, 111.

10. Moffitt, W. (1954) J. Chem. Phys., **22**,320.

11. Ellis, R. L., G. Kuehnlenz and H. H. Jaffe (1972) Theor. Chim. Acta, **26**, 131.

12. Sprecher, C. A., W. C. Johnson (1977) Biopolymers, **16**, 2243.

13. Mason, S. F. (1954) J. Chem. Soc. **54**, 2071.

14. Stewart, R. F., N. Davidson (1963) J. Chem Phys. **39**, 255.

15. Clark, L. B.(1989) J. Phys. Chem. **93**, 5345.

16. Anex, B. G., A. F. Fucaloro and A. Durra-Ahmed (1975) J. Phys, Chem., **79**, 2636.

17. Brown, J. N., L. M. Trefonas, A. F. Fucaloro and B. G. Amex (1974) J. Am. Chem. Soc., **96**, 1579.

18. Callis,P.R. and W. T. Simpson (1970) J.Am. Chen. Soc., **92**, 3593.

19. Lewis, T. P., W. A. Eaton (1971) J. Am. Chem. Soc., **93**, 2054.

20. Clark, L. B. (1977) J. Am. Chem. Soc., **99**, 3934.

21. Vigny, P., J. P. Ballini (1977) In Excited State in Organic Chemistry and Biochemistry, 1, D. Reidel Publishing Co., Boston.

22. Vigny, P., A. Favre (1974) Photochem. Photobiol, **20**, 345.

23. Vigny, P. (1973) CR Acad. SCi. Paris Ser. D, **277**, 1941.

24. Ballini, J. P., P. Vigny, G. Thomas and A. Favze (1976) Photochem. Photobiol, **24**, 321.

25. Callis, P. R., B. Fanconi and W. T. Simpson (1971) J. Am. Chem. Soc., **93**, 6679.

26. Matsuoka, Y. and B. Norden (1982) J. Phys. Chem., **86**, 1378.

27. Leng, M., F. Pochon and A. M. Michelson (1968) Biochim. Biophys. Acta, **169**, 338.

28. Georghiou, S. and A. M. Saim (1986) Photochem. Photobiol., **44**, 733.

29. Parker, C. A. (1968) Photoluminescence of Solutions, Elsevier, New Youk.

30. Hendler, S., E. Furer and P. R. Scrinivasan (1970) Biochemistry, **9**, 4141.

31. Callis, P. R. (1979) Chem. Phys. Lett., **61**, 563.

32. Perrin, F. (1929) Ann. Phys. (Paris) **12**, 169.

33. Jablonski, A. (1935) Z. Physik, **96**, 236.

34. Georghiou, S., T. M. Nordlund and A. M. Saim (1985) Photochem. Photobiol., **41**, 209.

35. Demchenko, A. P. and A. S. ladokhin (1988) Eur. Biophys. J., **15**, 69.

36. Tao, T. (1969) Biopolymers, **8**, 609.

37. Hofrichter, J. and W. A. Eaton (1976) Ann. Rev. Biophys. Bioeng., **5**, 511.

38. Norden, B. (1978) Appl. Spectrosc. Rev., **14**, 157.

39. Ito, H. and Y. J. I'Haya (1976) Bull. chem. soc. Jpn., **49**, 3466.

40. Hug, W. and I. Tinoco (1973) J. Am. Chem. Soc., **95**, 2803.

41. Danilov, V. I., V. I. Pechenaya,and N. v. Zheltovsky (1980) Int. J. Quantum Chem., **17**, 307.

42. Srivastava, S. k. and P. C. Mishra (1980) Int. J. Quantum Chem., **18**, 827.

43. Birks, J. B.(1970) Photophysics of Atomatic Molecules, John Wiley, New Youk.

44. Cech, C. L. and I. Tinoco (1977) Biopolymers, **16**, 43.

45. William, A. L. and D. S. Moore (1983) Biopolymers, **22**, 755.

46. Wang, H. -J., G. J. Quigley, F. J. Kolpak, J. L. Crawford, J. H. Van Boom, G. vam der Marel amd A. Rich (1979) Nature, **282**, 680.

47. Voet, D., W. D. Gratzer, R. A. Cox and P. Dotty (1963) Biopolymers, **1**, 193.

48. Förster, Th. (1968) Energetics and Mechanisms in Radiation Biology, PP. 183. Academic press, New Youk.

49. Gueron, M. and R. G. Shulman (1968) Ann. Rev. Biochemistry, **37**, 571.

50. Shafranovskaya, N. N., E. N. Trifonov, Y. S. Lazurkin and M. D. Frank-Kamenetskii, (1973) Nature New Biol. **241**, 58.

51. Brunk, C. F., (1973) Nature New Biol. **241**, 74.

52. Frank-Kamenetskii M. D. and Y. S. Lazurkin, (1974) Ann. Rev. Biophys. Bioeng. **3**, 127.

53. Ramstein, J., C. Helene and M. Leng, (1971) Eur. J. Biochem. **21**, 125.

54. Bauer, E., H. Berg, G. Lober, K. Weller, M. Hartmann and .3inCh. Zimmer, (1974) Biophys. Chem. **1**, 338.

55. Förster, Th. (1975) Mondern Quantum Chemistry 3, (Ed. O. Sinanoglu), Academic Press, NY.

56. Dexter, D. L. (1953) J. Chem. Phys. **21**, 836.

57. Borresen, H. Ch. (1967) Acta Chim. Scand. **21**, 2463.

58. Shapiro, H. S. and E. Chargaff, (1957) Biochim. Biophys. Acta **26**, 596.

59. Inman, R. B. and R. L. Baldwin, (1962) J. Mol. Biol. **5**, 172.

60. P-L Biochemicals, (1976) Ultraviolet Absorption Spectra of 5'-Ribonucleotides, Milwaukee.

61. Inman, R. B. and R. L. Baldwin, (1964) J. Mol. Biol. **8**, 452.

62. Riley, M., B. Maling and M. J. Chamberlin, (1966) J. Mol. Biol. **20**, 359.

63. Devie, H. (1969) Ann. N. Y. Acad. Sci. **158**, 298.

64. Gueron, M., J. Eisinger and R.G. Shulman, (1967) J. Chem. Phys. **47**, 4077.

65. Ballini, J. P., P. Vigny and M. Daniels, (1983) Biophys. Chem. **18**, 61.

66. Aoki, T. I. and P. R. Callis, (1982) Chem. Phys. Lett. **92**, 323.

67. Pohl, F. M., A. Ranade and M. Stockburger, (1973) Biochim. Biophys. Acta **335**, 85.

68. Kearns, D. R., P. A. mirau, N. Assa-Munt and D. W. Behling, (1983) Nucleic Acids: The Vectors of Life, R. Reidel Publishing Co., Boston.

69. Assa-Munt, N. and D. R. Kearns, (1984) Biochemistry **23**, 791.

70. Lang, H. (1975) Nucleic Acids Res. **2**, 179.

71. Rahn, R. O. (1976) Nucleic Acids Res. **3**, 876.

72. Setlow, R. B. and W. L. Carrier, (1966) J.Mol. Biol. **17**, 237.

73. Turpin, P. -Y., W. L. Peticolas (1985) J. Phys. Chem., **89**, 5156.

74. Hart, L. P., M. Daniels (1989) Biochem. Biophys. Res. Commun. **162**, 781.

75. Förster, Th. (1959) Discussions Faraday Soc. **27**, 7.

76. Daniels, M. (1970) Physicochemical Properties of Nucleic Acids, Vol. 1, J. Duchesne, Academic Press, NY.

77. Anders, A. (1981) Chem. Phys. Lett. **81**, 270.

78. Azumi, T. and H. Azumi, (1966) Bull Chem. Soc. Jpn. **39**. 1829.

79. Vala, M. T., J. Haebig and S. A. Rice, (1965) J. Chem. Phys. **43**, 886.

80. Wang,Y. -C. and H. Morawetz, (1975) Macromolekulare Chemie, Suppl. **1**, 283.

81. Zachariasse, K. and W.Kuhnle, (1976) Z. Physik. Chemie N. F., **101**, 267.

82. Edward, J. T., (1970) J.Chem. Ed. **47**, 261.

83. Förster, Th. (1960) Comparative Effects of Radiation, Wiley, New York.

84. Voltz, R. (1960) Radiation Res. Revs. **1**, 301.

85. Simpson, W. T. and D. L. Peterson, (1957) J. Chem. Phys. **26**, 588.

86. Siebrand, W. (1969) J. Chem. Phys. **50**, 1040.

87. Holzwarth, A. R., K. Razi Naqvi and U.P. Wild, (1977) Chem. Phys. Lett. **46**, 473.

88. Razi Naqvi, K. (1980) Photochem. Photobiol. **31**, 523.

89. Sommer and J.Jortner, (1968) J. Chem. Phys., **49**, 3919.

90. Jortner, J., S. A. Rice, J. J. Katz, and S. -I. Choi, (1965) J. Chem. Phys. **42**, 309.

91. Asami, H., T. Nakayama, T. Chong and N. Itoh, (1978) Phys. Stat. Sol. **88b**, 623.

APPENDIXES

Appendix I

Fraction of light f_a absorbed by state I at 290, 260 and 244 nm for a number of different values for θ, the angle between the absorption transition dipole moments of states I and II. The emission anisotropy, r_b, for state II was obtained from Eq. 2.8.

θ	r_b	f_a		
		290	260	244
90°	-0.040	0.842	0.613	0.696
80°	-0.036	0.835	0.599	0.685
70°	-0.026	0.821	0.561	0.656
60°	-0.010	0.789	0.483	0.594
50°	0.010	0.729	0.336	0.479
46°	0.018	0.694	0.250	0.411
43°	0.024	0.661	0.170	0.348
40°	0.030	0.620	0.070	0.270

Appendix II

Values of the distances R(Å), upper, and the square of the orientational factor k, lower, for adjacent bases in the DNA double helix for intrastrand transfer. The direction of the transition dipole moments were obtained from the literature (see text).

Acceptor ↓ 5′	→ 3′ Donor			
	A	T	C	G
A	3.9 0.51	4.4 0.76	4.1 0.79	3.9 0.56
T	3.8 0.07	4.1 0.03	3.8 0.1	3.7 0.16
C	4.0 0.18	4.4 0.19	4.1 0.59	3.9 0.23
G	4.0 0.002	4.4 0.07	4.2 0.26	3.9 0.17
MeG	4.0 0.002	4.4 0.07	4.2 0.26	3.9 0.17

Appendix III

Spectral overlap J (10^{-17} cm^3 M^{-1}) for the different adjacent donor-acceptor pairs. For the cases in which A is the acceptor or MeG (the trap) is the donor, the values of J were found to be very small and are omitted from the table.

Acceptor	Donor			
	A	T	C	G
T	9.6	1.6	1.3	1.7
C	12.2	2.2	1.8	2.1
G	19.0	3.9	3.7	3.5
MeG	57.8	27.1	22.8	13.3

Appendix IV

Comparison of the experimental and simulated values of the efficiency f of energy transfer from the other bases to the trap for methylated calf thymus DNA for differently assumed values of the fluorescence quantum yield ϕ_o of A and T, C, and G. (A) $\phi_{oA} = \phi_{oT,C,G} = 3 \times 10^{-4}$; (B) $\phi_{oA} = 1 \times 10^{-6}, \phi_{oT,C,G} = 1 \times 10^{-3}$; (C) $\phi_{oA} = 1 \times 10^{-5}, \phi_{oT,C,G} = 2 \times 10^{-3}$; (D) $\phi_{oA} = 1 \times 10^{-6}, \phi_{oT,C,G} = 2 \times 10^{-3}$; (E) $\phi_{oA} = 1 \times 10^{-6}, \phi_{oT,C,G} = 3 \times 10^{-3}$. The excitation wavelenth is designated by λ.

λ(nm)	f (experimental)	f(simulated)				
		A	B	C	D	E
255	0.16	0.25	0.19	0.26	0.22	0.23
260	0.22	0.25	0.20	0.26	0.23	0.24
265	0.24	0.25	0.22	0.28	0.25	0.26
270	0.27	0.26	0.25	0.31	0.29	0.30
275	0.33	0.27	0.29	0.35	0.34	0.35
280	0.35	0.27	0.33	0.39	0.38	0.40
285	0.43	0.28	0.37	0.43	0.43	0.44
290	0.42	0.28	0.38	0.44	0.44	0.46
295	0.47	0.27	0.37	0.43	0.44	0.46

Appendix V

Critical transfer distances R_o (in Å) for intrastrand transfer between all the possible combinations of nearest neighbors in methylated DNA for $\phi_{oT,C,G} = 2 \times 10^{-3}$. The box at the lower right-hand corner indicates the direction of transfer. For each donor-acceptor pair the upper left-hand value refers to transfer in the 3′ to 5′ direction, whereas the lower right-hand value refers to transfer in the 5′ to 3′ direction. For the cases in which the trap (MeG) or A are the donors or when A is the acceptor, the values of R_o were found to be very small and are omitted from the table.

5′ → / 3′ ↓	T	C	G	MeG
T	3.0	4.4 / 4.0	4.1 / 3.6	5.7 /
C	3.6 / 3.9	5.2	5.1 / 4.6	6.8 /
G	4.1 / 4.7	4.5 / 5.0	4.7	5.9 /
MeG	/ 6.5	/ 6.7	/ 5.9	

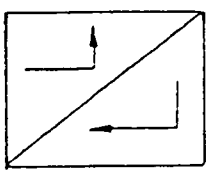

APPENDIX VI
FIGURES

Figure 1.

Steady-state fluorescence anisotropy of 7-methyl GMP in 0.05 M sodium cacodylate, 0.1 M NaCl, pH 5 at room temperature as a function of excitation wavelength. The anisotropy has been found to be independent of the emission wavelength. The bars on one of the points indicate the standard deviation.

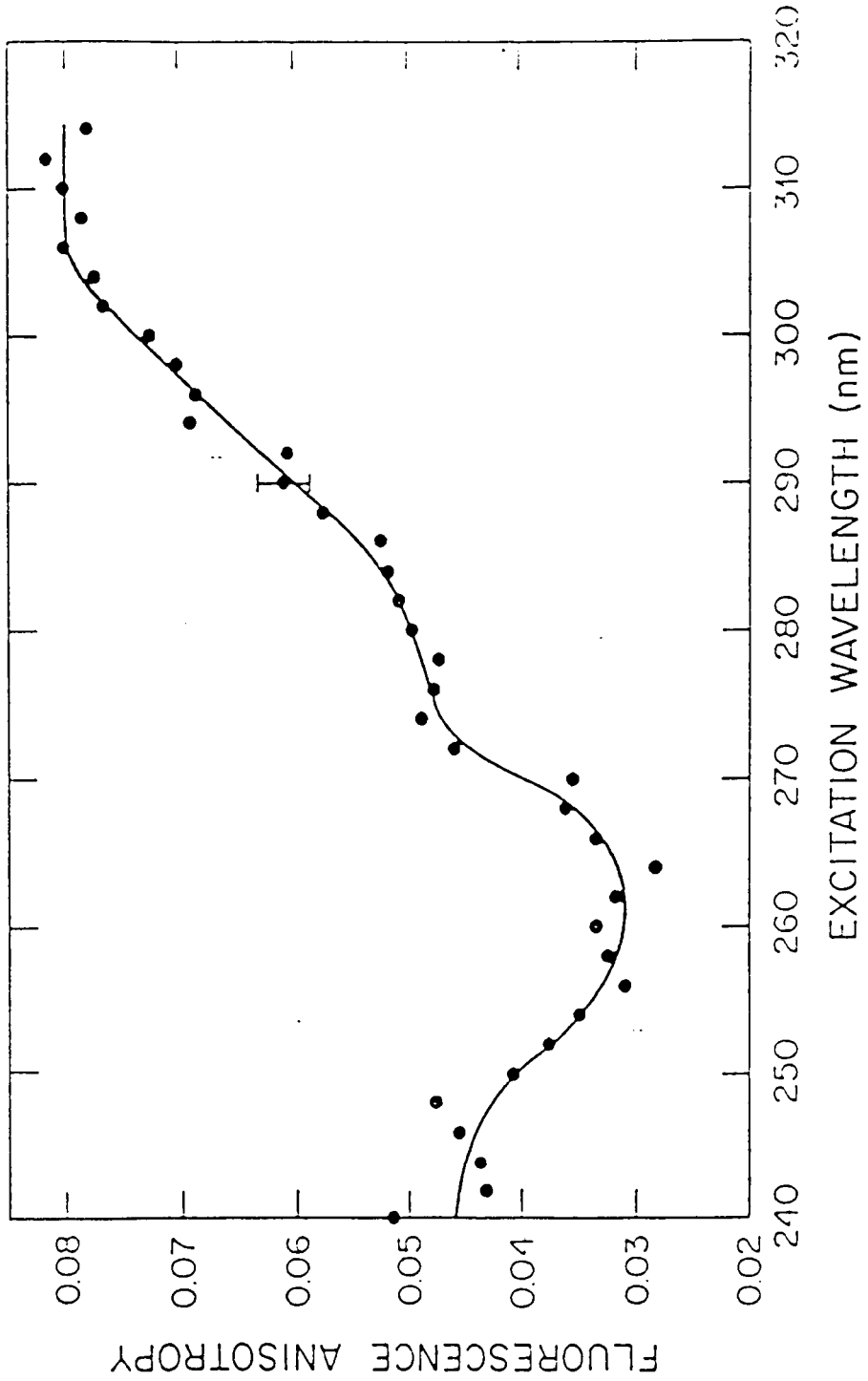
FLUORESCENCE ANISOTROPY
0.08
0.07
0.06
0.05
0.04
0.03
0.02
240
250
260
270
280
290
300
310
320
EXCITATION WAVELENGTH (nm)

Figure 2.

Relative fluorescence quantum yield of 7-methyl GMP in 0.05 M sodium cacodylate, 0.1 M NaCl, pH 5 at room temperature as a function of excitation wavelength. The yield has been found to be independent of the wavelength at which the emission was monitored.

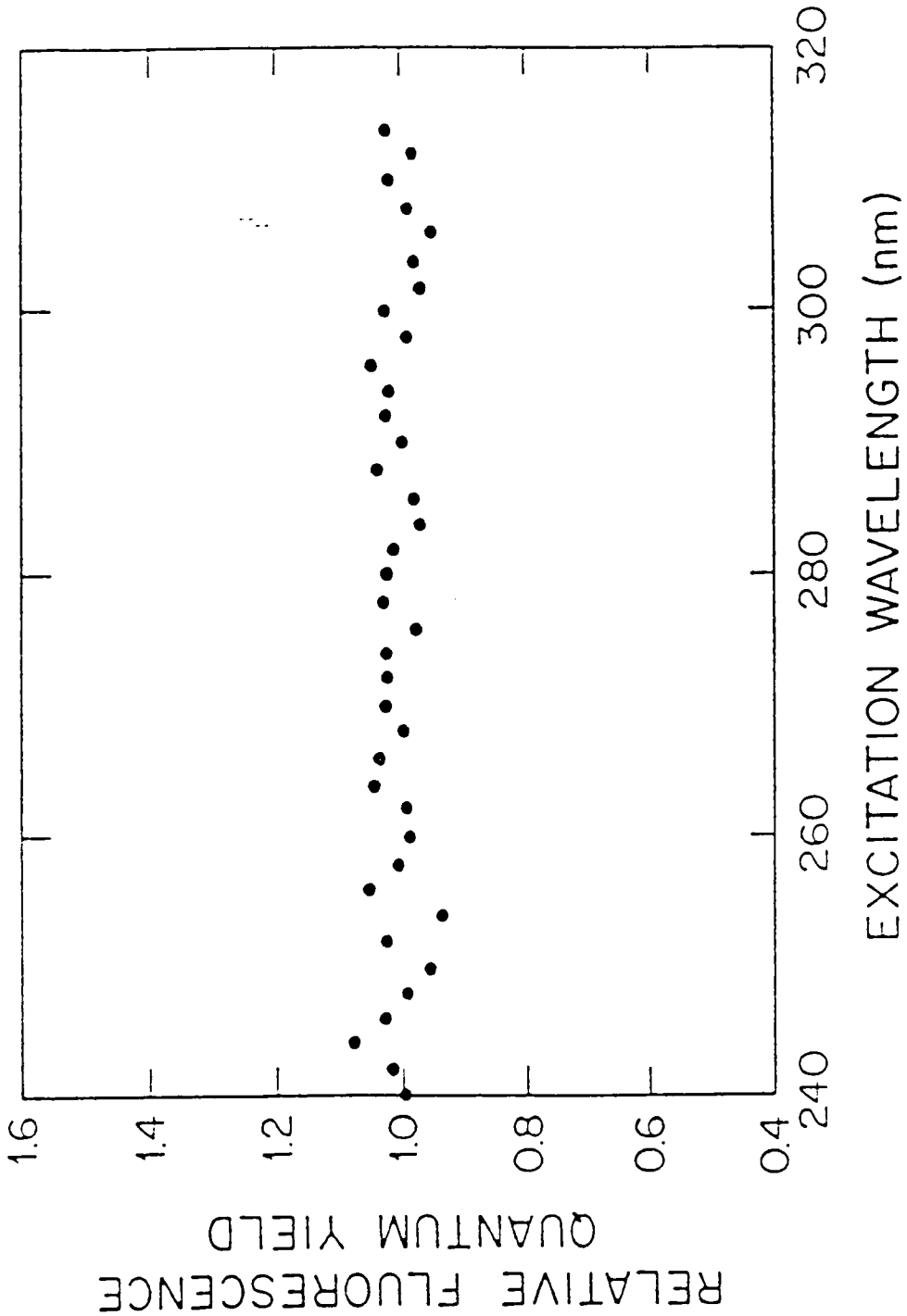
RELATIVE FLUORESCENCE
QUANTUM YIELD
1.6
1.4
1.2
1.0
0.8
0.6
0.4
240
260
280
300
320
EXCITATION WAVELENGTH (nm)

Figure 3.

Fluorescence spectrum of 7-methyl GMP in 0.05 M sodium cacodylate, 0.1 M NaCl, pH 5 at room temperature. The spectrum has been found to be independent of the excitation wavelength when exciting in the 240 to 310 nm spectral range.

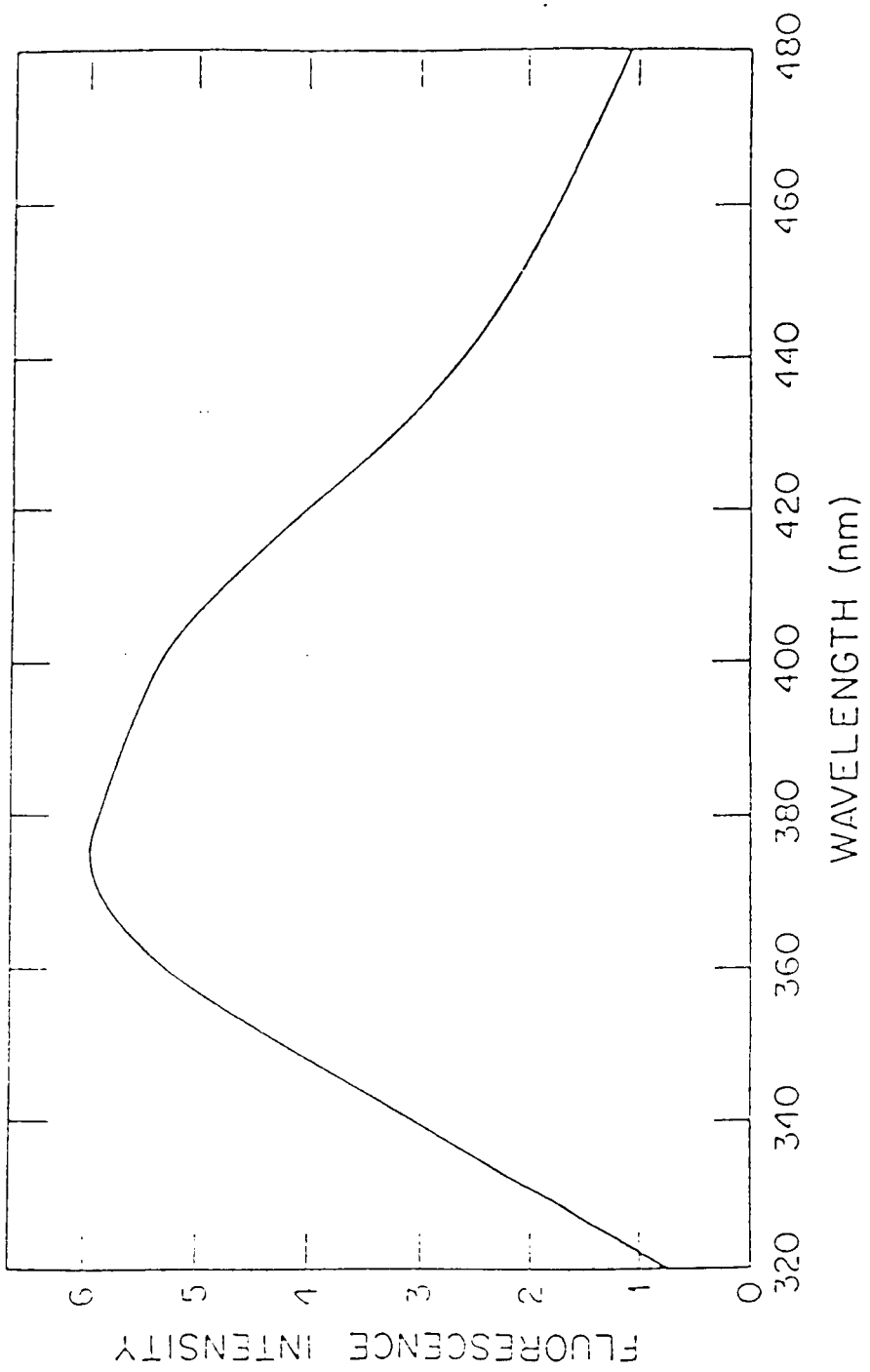
FLUORESCENCE INTENSITY
0
1
2
3
4
5
6
320
340
360
380
400
420
440
460
480
WAVELENGTH (nm)

Figure 4.

Absorption spectrum of 7-methyl GMP in 0.05 M sodium cacodylate, 0.1 M NaCl, pH 5 at room temperature (full line) and component spectra for band I (•) and band II (○) for $\theta = 70^{o}$, where θ is the angle between the absorption transition dipole moments of states I and II. This figure illustrates how the spectra look when absorption by state I predominates across the total wavelength range. This is contrary to the conclusion of previous studies of single-crystal polarized reflection[24,25] and linear dichroism from stretched films (Matsuoka and Norden, 1982), according to which for guanine and some of its derivatives in the short-wavelength region state II is the predominantly absorbing state. Figure 5 illustrates how the total absorption spectrum is resolved into the constituent absorption spectra for states I and II in a manner which is in accord with these published findings. (Such an agreement is achieved for only a very limited range of θ values, $40^{o} \leq \theta < 50^{o}$.)

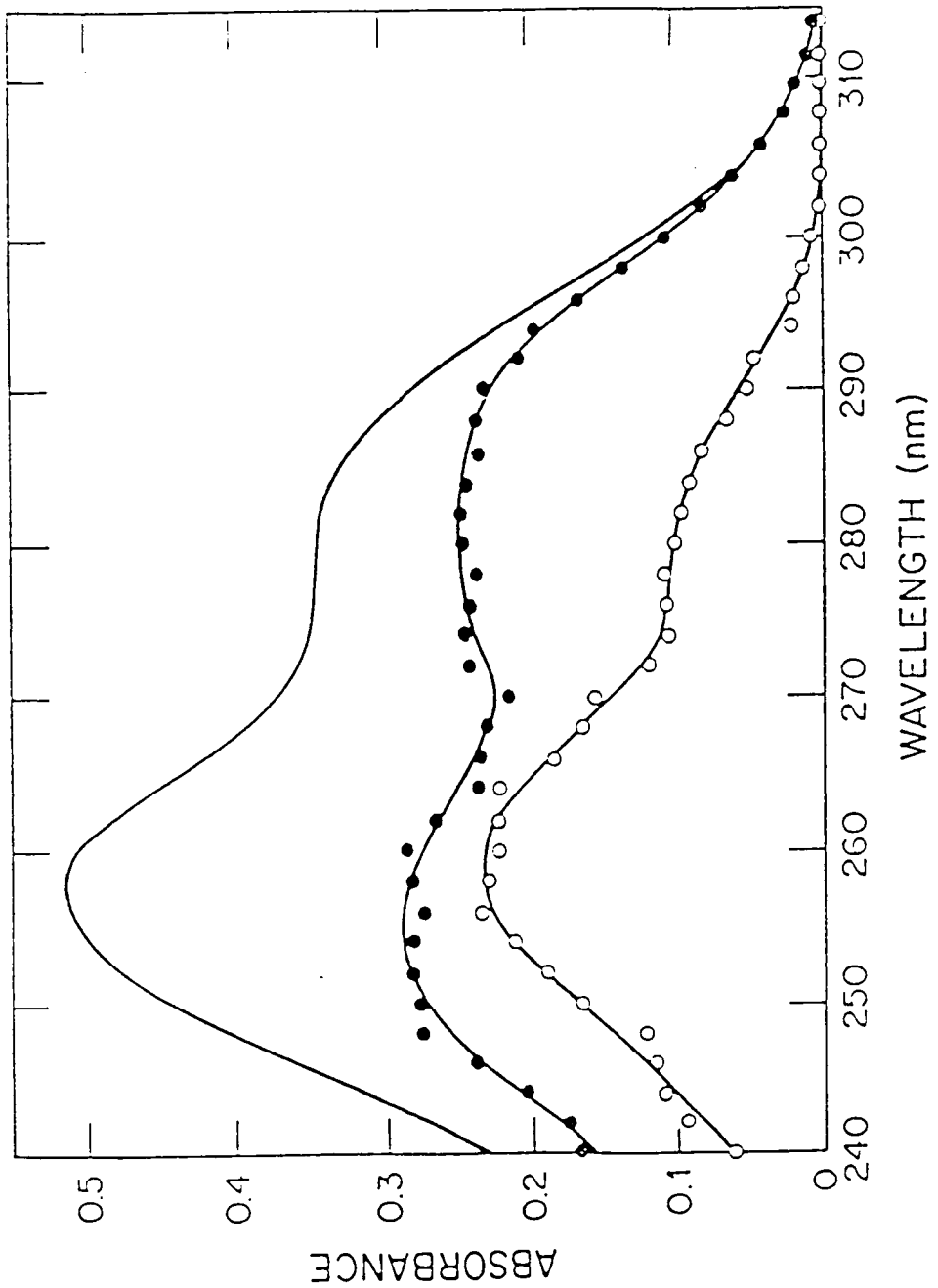
ABSORBANCE
0.5
0.4
0.3
0.2
0.1
0
240
250
260
270
280
290
300
310
WAVELENGTH (nm)

Figure 5.

Absorption spectrum of 7-methyl GMP in 0.05 M sodium cacodylate, 0.1 M NaCl, pH 5 at room temperature (full line) and component spectra for band I (•) and band II (○) for $\theta = 43^o$, where is the angle between the absorption transition dipole moments of states I and II. This angle was chosen because only for $40^o \leq \theta < 50^o$ does the resolution of the absorption spectrum agree with the conclusion of previous studies for guanine and some of its derivatives that, in the short-wavelength region, state II is the predominantly absorbing state. These studies involved single-crystal polarized reflection[21,23] and linear dichroism from stretched films.[22] The bars on one of the points indicate the standard deviation. Also shown with dashed lines is a graphical separation of the absorption spectrum of state I from that of a band that appears at short wavelengths. (This was done simply to obtain an estimate of the contribution of the latter to the total absorption.)

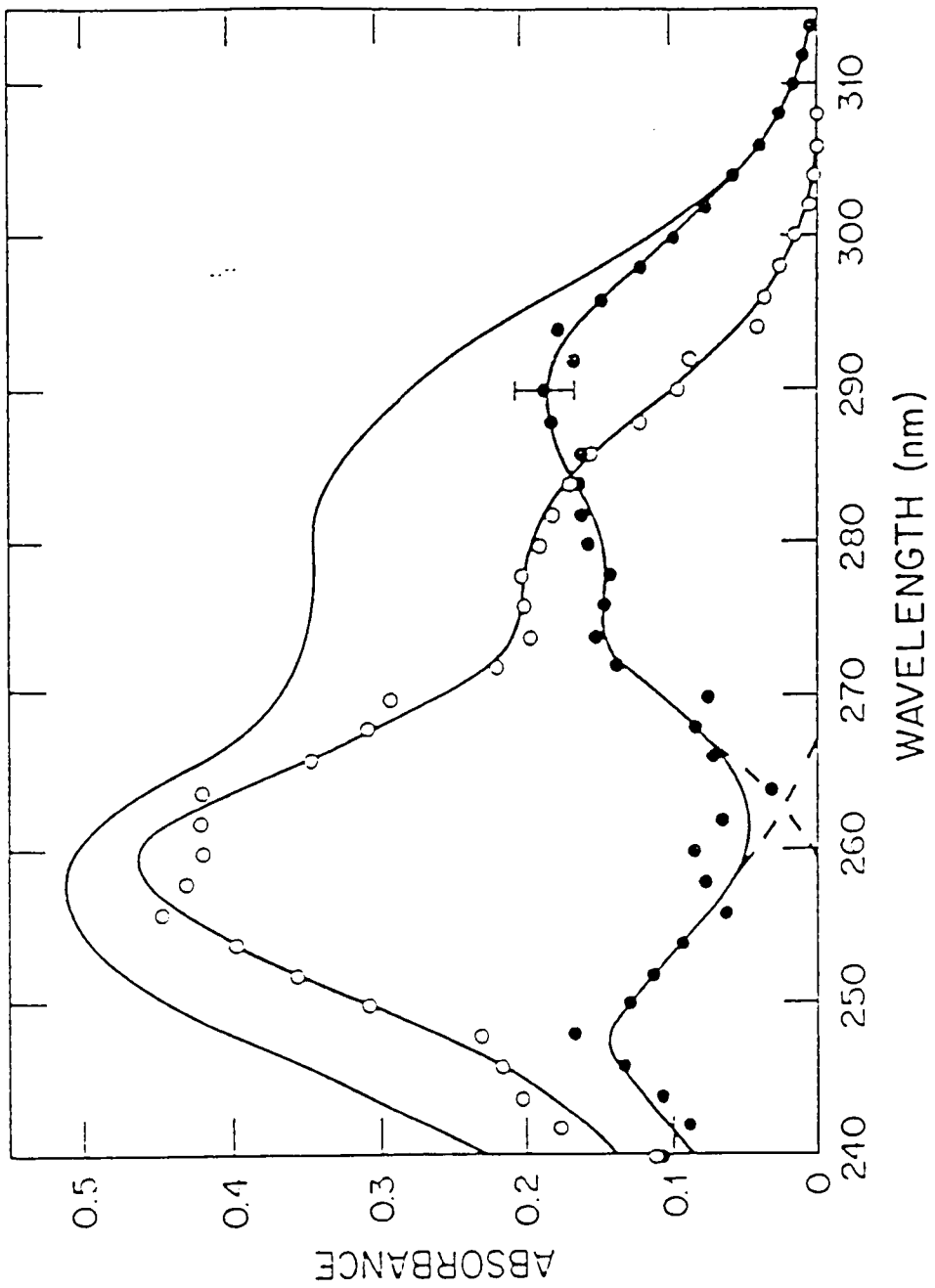
ABSORBANCE
0.5
0.4
0.3
0.2
0.1
0
240
250
260
270
280
290
300
310
WAVELENGTH (nm)

Figure 6.

Fluorescence quantum yield (•) of methylated calf thymus DNA in 0.05 M sodium cacodylate, 0.01 M NaCl, pH 6.6 in triply distilled water at room temperature, Also shown is the product α q (o), where α is the fraction of light absorbed by the trap (methylated guamine) and q is its fluorescence quantum yield: these are the expected values when there is no energy transfer from the other bases to the trap.

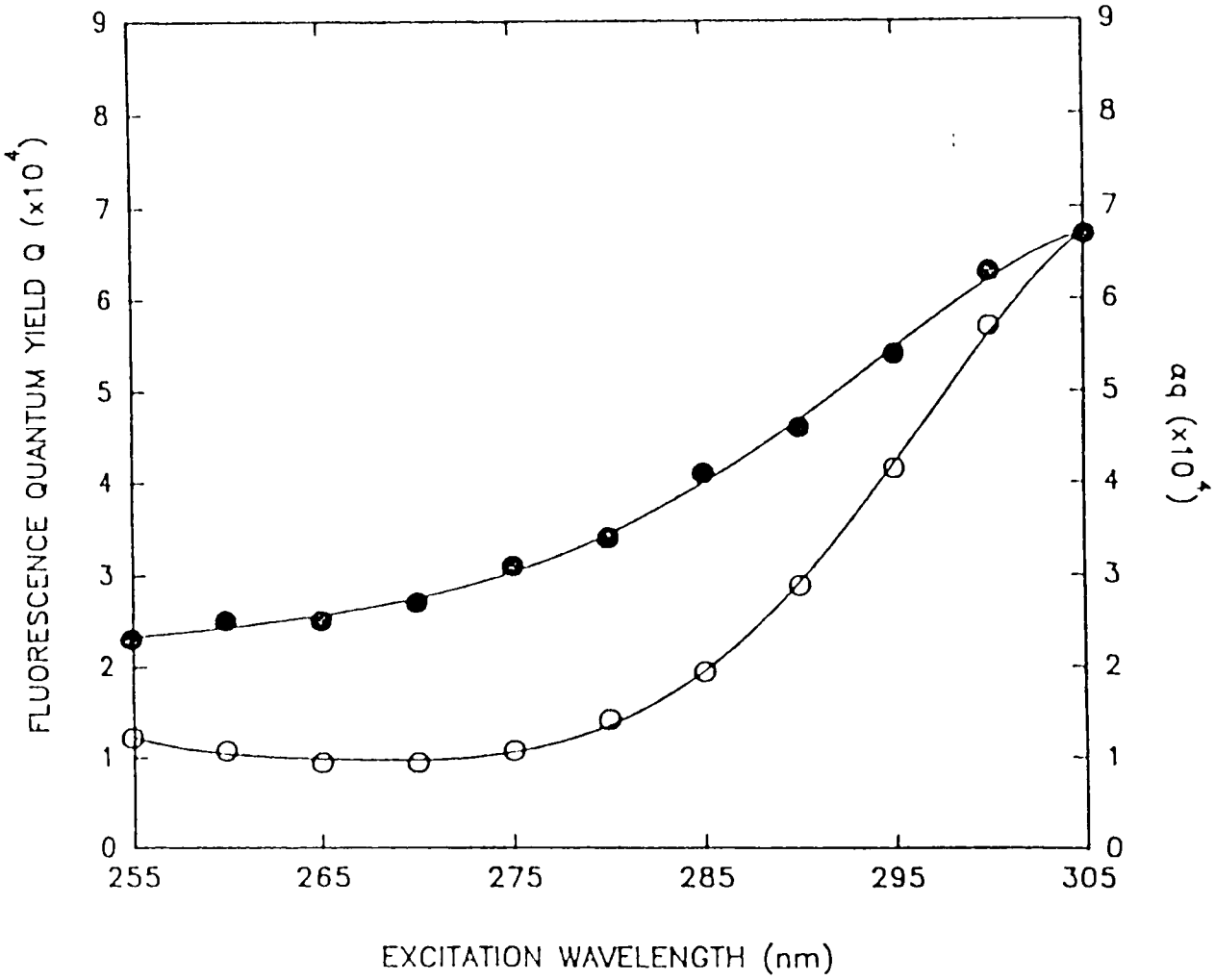
FLUORESCENCE QUANTUM YIELD Q (x10^{4})
α_B (x10^{4})
EXCITATION WAVELENGTH (nm)
0
1
2
3
4
5
6
7
8
9
255
265
275
285
295
305

Figure 7.

Efficiency f of energy transfer from the other bases to the trap calculated by using Equation (3.3) that omits emission from the other bases (•) and by using Equation (3.4) that takes into account such emission (o). Also shown are the simulated values of f (□) obtained by using a stochastic model, which employs the dipole-dipole term in the interaction potential for the coulombic interaction, to calculate the rate constant of transfer. The fraction of light absorbed by the A bases is also plotted (■).

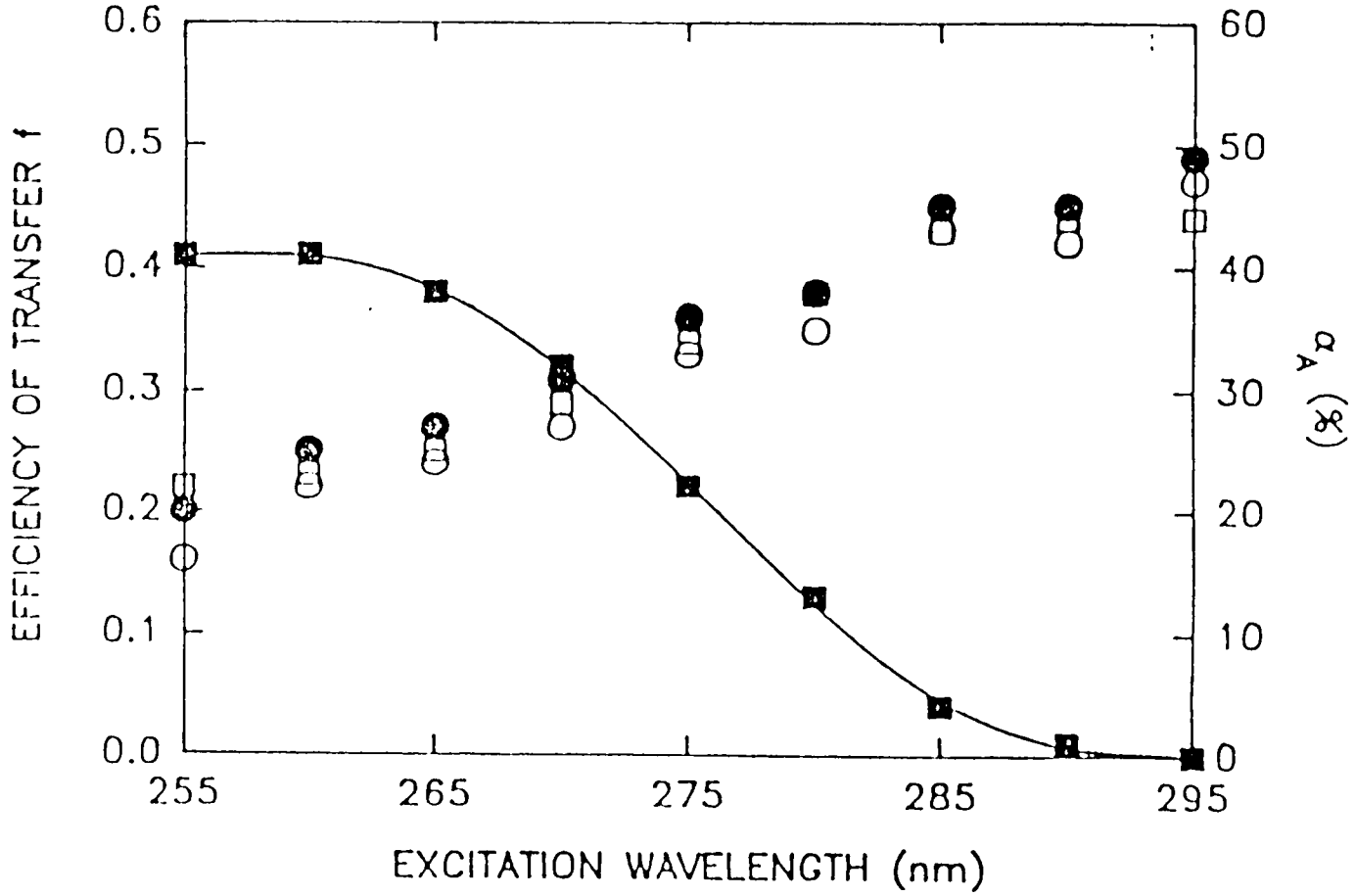
EFFICIENCY OF TRANSFER f
0.6
0.5
0.4
0.3
0.2
0.1
0.0
255
265
275
285
295
EXCITATION WAVELENGTH (nm)
60
50
40
30
20
10
0
α_A (%)

Figure 8.

Transfer paths considered during the simulations by using a stochastic model that employs the dipole-dipole term in the interaction potential for the coulombic interaction to calculate the rate constant of transfer. The initially excited base is denoted by i_o and the trap by $i_n = 0$. Positive and negative values indicate the sequence of bases in the direction of the trap and in the opposite direction, respectively, along the same strand. In the simulations we have also included interstrand transfer (for which i_b designates a base hydrogen bonded to a C); we have found that C-trap transfer is the only interstrad transfer that makes a significant contribution to the efficiency of trapping (see text).

TRANSFER PATHS

No. of steps

1:

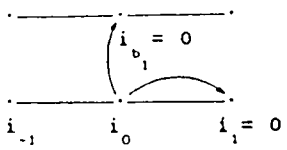

2:

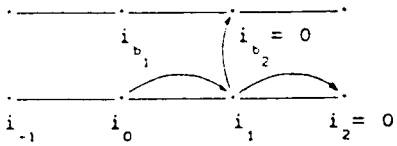

3:

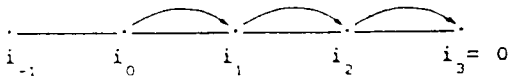

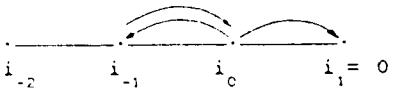

4:

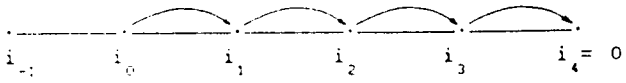

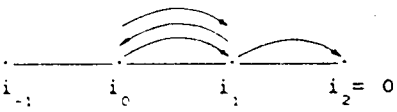

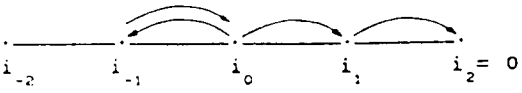

VITA

Shen Zhu was born in Shanghai, China on April 11,1953. In the Fall of 1978 he enrolled at the Huazhong University, China. After he graduated with a Bachelor degree with a major in Physics in 1982, he became a teacher in the Department of Physics of Huazhong University. He became a graduate student with a major in Computer Science in 1985. He came the U.S.A. as a visiting scholar in November,1986. He accepted a teaching assistantship at the University of Tennessee, Knoxville in the Fall of 1987. He received the Master of Science degree with a major in Physics in December 1990. Mr. Shen Zhu is working on a Doctor of Philosophy degree.